

High-potassium, calc-alkaline I-type plutonism in the European Variscides: northern Vosges (France) and northern Schwarzwald (Germany)

Rainer Altherr^{a,*}, Albert Holl^b, Ernst Hegner^c, Carola Langer^{a,1}, Hans Kreuzer^{d,2}

^a Mineralogisches Institut, Universität Heidelberg, Im Neuenheimer Feld 236, D-69120 Heidelberg, Germany

^b Mineralogisches Institut, Universität Karlsruhe (TH), Kaiserstraße 12, D-76131 Karlsruhe, Germany

^c Institut für Mineralogie, Petrologie und Geochemie, Universität Tübingen, Wilhelmstraße 56, D-72074 Tübingen, Germany

^d Bundesanstalt für Geowissenschaften und Rohstoffe, Stilleweg 2, D-30655 Hannover, Germany

Received 20 April 1999; accepted 6 August 1999

Abstract

Early Carboniferous high-K, calc-alkaline I-type plutonic rocks from the northern Vosges and Schwarzwald were studied for their chemical and Sr–Nd isotopic compositions. Intrusion relationships and mineralogical and chemical characteristics allow to distinguish four suites. The oldest intrusions are diorites (1), followed by a granodioritic (2) and a granitic (3) suite. These older granitoids (OG) and their contact metamorphic country rocks are cut by younger high-K to shoshonitic granitic plutons (YG) (4). Still later, peraluminous S-type granitic magmas intruded (not included in this study). Diorites (1) have SiO₂ between 46 and 61 wt.% and are characterized by relatively high Mg# of 62–38, low contents of Na₂O (2.3–4.0 wt.%), high abundances of incompatible elements (LILE, Nb, and P) and enriched Nd–Sr initial isotopic signatures [$\varepsilon_{\text{Nd}}(\text{I}) = -1.7$ to -2.8 ; $^{87}\text{Sr}/^{86}\text{Sr}(\text{I}) = 0.7046\text{--}0.7061$]. Chondrite-normalized (cn) REE patterns are relatively flat [$(\text{La}/\text{Yb})_{\text{cn}} = 5.1\text{--}7.8$; $(\text{Tb}/\text{Yb})_{\text{cn}} = 1.2\text{--}1.8$] and show small negative Eu anomalies ($\text{Eu}/\text{Eu}^* = 0.73\text{--}0.90$). All these characteristics suggest an origin of the diorites from enriched lithospheric mantle sources. Compared with the diorites, the granodiorites (2) show higher $\varepsilon_{\text{Nd}}(\text{I})$ (+0.5 to -0.4) but similar $^{87}\text{Sr}/^{86}\text{Sr}(\text{I})$ (0.7051–0.7053). High values of molar $\text{CaO}/(\text{MgO} + \text{FeO}_{\text{tot}})$ combined with low $\text{Al}_2\text{O}_3/(\text{MgO} + \text{FeO}_{\text{tot}})$ and $\text{K}_2\text{O}/\text{Na}_2\text{O}$ ratios suggest an origin by dehydration melting from a metabasaltic to metatonalitic source. Radiogenic isotopic signatures of the older granites (3) are similar to those of the diorites [$\varepsilon_{\text{Nd}}(\text{I}) = -1.8$ to -2.5 ; $^{87}\text{Sr}/^{86}\text{Sr}(\text{I}) = 0.7048\text{--}0.7058$]. Compared with the granodiorites the older granites show similar values of $\text{CaO}/(\text{MgO} + \text{FeO}_{\text{tot}})$, but significantly higher ratios of $\text{Al}_2\text{O}_3/(\text{MgO} + \text{FeO}_{\text{tot}})$ and $\text{K}_2\text{O}/\text{Na}_2\text{O}$ pointing to a metagreywacke source. REE patterns of both the granodiorites and the granites are characterized by relatively low $(\text{Tb}/\text{Yb})_{\text{cn}}$ ratios (1.2–1.7) excluding substantial amounts of garnet as a fractionating phase. Instead, the residues were probably dominated by amphibole and plagioclase, and possibly also pyroxene. The YG (4) have elevated abundances of large ion lithophile elements (K, Rb, Th, U, Ba, and Sr) and of some high field strength elements (Nb and P). Their isotopic signatures [$\varepsilon_{\text{Nd}}(\text{I}) = -1.5$ to -3.4 ; $^{87}\text{Sr}/^{86}\text{Sr}(\text{I}) = 0.7046\text{--}0.7060$] are similar to those of the older granites.

* Corresponding author. Tel.: +49-6221-548-206; fax: +49-6221-544-805; e-mail: raltherr@classic.min.uni-heidelberg.de

¹ Now at: Institut für Festkörper- und Werkstofforschung, Helmholtzstraße 20, D-01069 Dresden, Germany.

² Now at: Hamsunstraße 19, D-30655 Hannover, Germany.

Relative to all OG, their REE patterns are characterized by higher ratios of $(\text{La}/\text{Yb})_{\text{cn}}$ (11.8–38.9) and $(\text{Tb}/\text{Yb})_{\text{cn}}$ (1.3–2.6) but lower values of Eu/Eu^* . Combined with higher $\text{Mg}\#$ and lower abundances of Y, these characteristics point to an increasing role of garnet in the residues of the partial melts. Relatively low values of molar $\text{Al}_2\text{O}_3/(\text{MgO} + \text{FeO}_{\text{tot}})$ and $\text{K}_2\text{O}/\text{Na}_2\text{O}$ in combination with variable molar $\text{CaO}/(\text{MgO} + \text{FeO}_{\text{tot}})$ ratios suggest that these magmas were derived from heterogeneous metasedimentary sources. © 2000 Elsevier Science B.V. All rights reserved.

Keywords: European Variscides; Vosges; Schwarzwald; Mid-German crystalline rise; Granitoid genesis; High-K granitoids; Saxothuringian zone

1. Introduction

Granitoid plutons form essential constituents of collisional belts. Their large compositional diversity arises from (1) different source compositions, (2) variable melting conditions, (3) complex chemical and physical interactions between mafic and felsic magmas and (4) crustal contamination (e.g., Zorpi et al., 1989, 1991; Patiño Douce, 1996; Petford et al., 1996; Poli et al., 1996). It has been suggested that tonalitic to granitic calc-alkaline magmas may be generated by dehydration melting of fertile portions of the continental crust at temperatures above $\sim 780^\circ\text{C}$ (e.g., Wolf and Wyllie, 1994; Rapp, 1995; Rapp and Watson, 1995; Patiño Douce, 1996; Patiño Douce and Beard, 1996; Patiño Douce and McCarthy, 1998; Thompson, 1996; and references therein). Calculated pressure–temperature–time (P – T – t) paths for continental collision (e.g., Brown, 1993; Thompson and Connolly, 1995) have shown that temperatures in excess of 780°C within the continental crust require unusual tectonic circumstances, such as slow exhumation allowing for long-time heating (see Patiño Douce and McCarthy, 1998 for discussion). This has led several authors to propose an advective input of heat from the mantle into the continental crust (e.g., Huppert and Sparks, 1988; Bergantz, 1989; Roberts and Clemens, 1993; von Blanckenburg et al., 1998). Furthermore, the ubiquitous occurrence of mafic (i.e., dioritic to gabbroic) rocks as microgranular enclaves in more felsic hosts or as separate intrusive bodies suggests a direct chemical input from the mantle, since extremely high temperatures in excess of $\sim 1100^\circ\text{C}$ must be achieved to generate such magmas by H_2O -undersaturated partial melting of mafic crustal source rocks (e.g., Rapp, 1995; Rapp and Watson, 1995; Patiño Douce and McCarthy, 1998).

In many cases, mafic plutonic rocks associated with more felsic granitoids display enriched chemical and Nd–Sr isotopic signatures (e.g., Pin et al., 1990; Allen, 1991; Holden et al., 1991; Janousek et al., 1995; Metcalf et al., 1995; Elburg, 1996; Galán et al., 1996; von Blanckenburg et al., 1998) compatible with an origin from lithospheric rather than depleted asthenospheric mantle sources. It has been shown that intensive mass transfer between mafic globules and felsic host magma seems to be the rule rather than the exception (e.g., Vernon, 1990; Holden et al., 1991; Elburg, 1996; Petford et al., 1996) and rapid chemical and isotopic exchange between coexisting mafic and felsic magmas is also suggested by experimental evidence (e.g., Baker, 1989; van der Laan and Wyllie, 1993; Leshner, 1994). As a consequence, uncertainty as to the origin and significance of enclaves has led many investigators to ignore their potential value as documents of magma sources. Furthermore, mafic intrusions in collisional belts occur as sporadically distributed, late-stage K-rich (lamprophyric) dikes (e.g., Rock et al., 1986; Turpin et al., 1988; Janousek et al., 1995; von Blanckenburg et al., 1998) with no obvious genetic relationship to the main volume of granitoid rocks. Therefore, the question as to whether mantle-derived mafic magmas could form a significant mass portion of granitoid plutons in collisional belts remains a highly debated issue (e.g., Roberts and Clemens, 1993).

The internal domains of the European Variscides (Saxothuringian and Moldanubian zones of Kossmat, 1927; Fig. 1a) are characterized by exceptionally large volumes of early Carboniferous granitoid rocks whereby peraluminous (S-type) granites and granodiorites predominate and mafic intrusions are volumetrically insignificant (e.g., Didier, 1991; Sabatier, 1991; Holub et al., 1995; Finger et al., 1997; Schaltegger, 1997). This has led many authors to neglect a

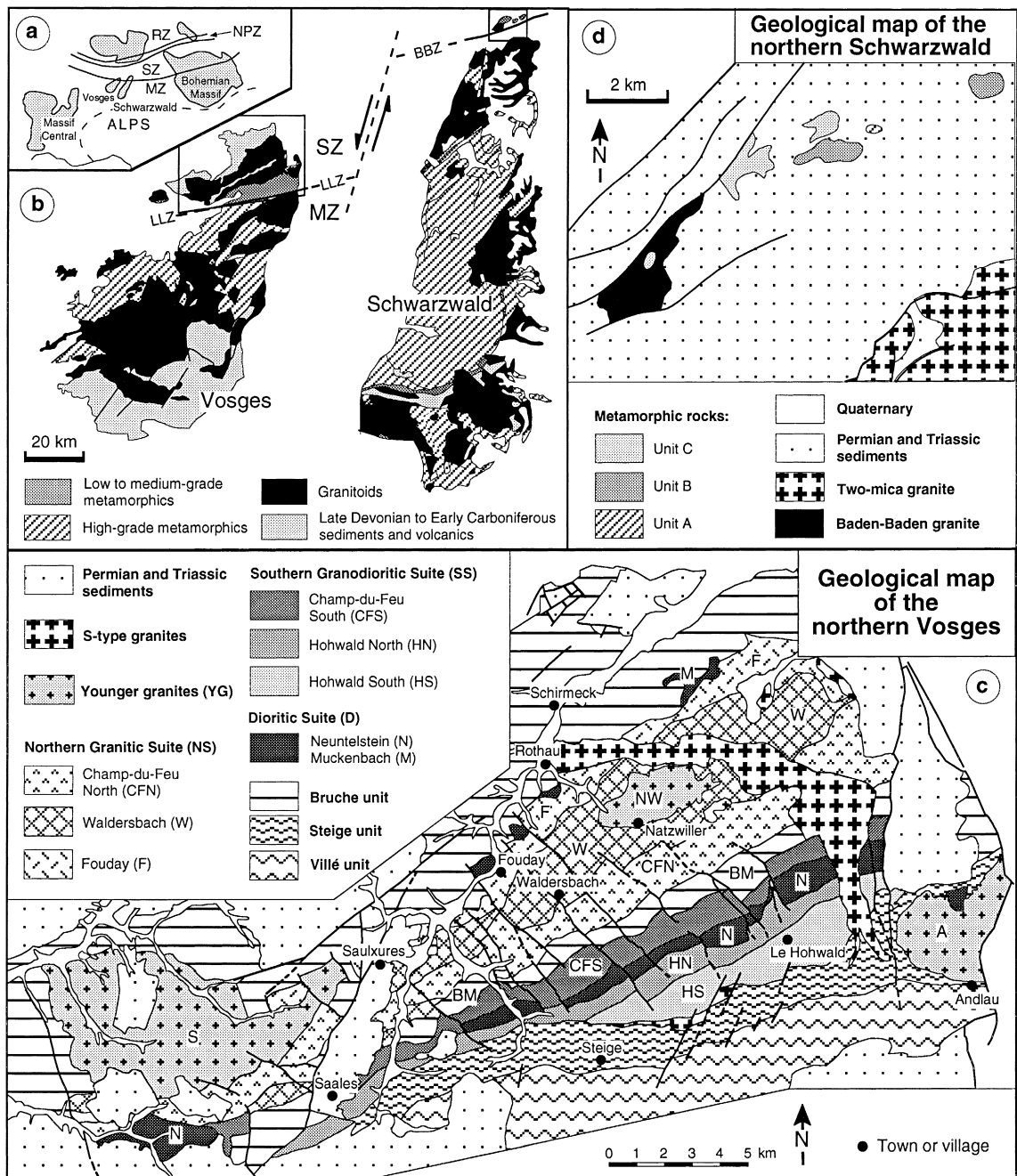


Fig. 1. (a) Sketch of the Central European Variscides showing the Rhenohercynian (RZ), Saxothuringian (SZ) and Moldanubian (MZ) zones of Kossmat (1927). NPZ, northern Phyllite zone. (b) Geological sketch map of Vosges and Schwarzwald with dextral shear zones of Lalaye–Lubine (LLSZ) and Baden–Baden (BBZ) representing the boundary between the Saxothuringian (SZ) and Moldanubian (MZ) zones. (c) Simplified geological map of the northern Vosges showing the various tectonic and intrusive units. The OG (D, SS, NS) form WSW–ENE elongated bodies, the YG show more isometric forms. These differences suggest a change in the crustal stress field after the intrusion of the OG and before the intrusion of the YG. (d) Geological map of the northern Schwarzwald showing the outcrops of metamorphic units A, B and C, the I-type granite of Baden–Baden and the two-mica (S-type) granite within Permian and Triassic sediments.

significant mass input from the mantle during granulite formation in this collisional belt (e.g., Hoefs and Emmermann, 1983; Bernard-Griffiths et al., 1985). On the other hand, mafic stocks and smaller plutons are relatively abundant in the more external Saxothuringian domain. Gabbroic and dioritic rocks from the Odenwald (Fig. 1), for example, have been interpreted as (subduction-related) mantle-derived melts that were partly modified by crustal contamination and magma mingling and mixing (Altherr et al., 1999). Dioritic rocks also form essential constituents of the northern Vosges where they are slightly older than, or contemporaneous with, associated I-type granodiorites and granites (von Eller, 1964, 1965, 1968, 1969; de Béthune et al., 1968). In this paper, we present new geochronological, geochemical and Sr–Nd isotopic data on post-collisional I-type granitoid plutons (high-K diorite to granite) from the northern parts of the Vosges and the Schwarzwald and we will use these data to constrain magma sources and magma producing processes.

2. Geological setting

2.1. General context

In the classic descriptions of the European Variscan Belt (Kossmat, 1927), the northern parts of the Vosges and the Schwarzwald have been assigned to the Saxothuringian Zone (Fig. 1a,b). In more recent concepts, this zone is thought to consist of various units that were derived from a northern lower and a southern upper plate and amalgamated during late Devonian to early Carboniferous oblique convergence and extension (e.g., Eisebacher et al., 1989; Oncken, 1997). Towards the south, the Saxothuringian units are in tectonic contact with high-grade gneisses and migmatitic rocks of the Moldanubian Zone (Fluck, 1980; Krohe and Eisebacher, 1988; Wickert and Eisebacher, 1988; Eisebacher et al., 1989; Fluck et al., 1989; Wickert et al., 1990; Ehtler and Altherr, 1993). To the north of the Saxothuringian Zone, low-grade high-pressure/low-temperature metamorphic rocks occurring in the northern Phyllite Zone and in the southern parts of the Rhenohercynian Zone document early Carboniferous southward-directed subduction processes

(Meisl et al., 1982; Ahrendt et al., 1983, 1996; Anderle et al., 1990; Meisl, 1990; Massonne, 1995; Ganssloser et al., 1996).

The northern parts of the Vosges and the Schwarzwald are characterized by an accretionary-wedge architecture with northwest-ward imbrication and superimposed dextral shear (Krohe and Eisebacher, 1988; Wickert and Eisebacher, 1988; Wickert et al., 1990; Eisebacher et al., 1989; Ehtler and Altherr, 1993). In the Vosges (Fig. 1b,c), the dextral shear zone of Lalaye–Lubine separates (very) low-grade metamorphic units of the Saxothuringian Zone in the north from high-grade metamorphic rocks of the Moldanubian Zone in the south (Fluck, 1980; Fluck et al., 1989; Wickert and Eisebacher, 1988). From south to north, the northern Vosges consist of the Villé unit, the Steige unit and the Bruche unit (Fig. 1c). The *Villé unit* is composed of low-grade metapelitic to metapsammitic schists and quartzites (Clauer and Bonhomme, 1970) deposited during late Cambrian to early Ordovician time (Reitz and Wickert, 1989 and references therein). The Villé unit is thrust over the *Steige unit* consisting of monotonous low-grade metapelites (Clauer and Bonhomme, 1970) that were deposited in a shallow marine environment during Ordovician to Silurian time (Doubinger, 1963; Tobschall, 1975; Müller, 1989). The *Bruche unit* is a sedimentary and tectonic *mélange* comprising middle Devonian to early Carboniferous shelf and slope sediments and calc-alkaline volcanic rocks (Rizki and Baroz, 1988; Wickert and Eisebacher, 1988; and references therein). The (very) low-grade Paleozoic volcano-sedimentary sequences were intruded by various plutons of dioritic to granitic compositions causing contact metamorphism (de Béthune et al., 1968; von Eller et al., 1971b; Leterrier, 1978).

In the northern Schwarzwald (Fig. 1b,d), three tectonic units of different structural and metamorphic evolution have been distinguished (Wickert et al., 1990). *Unit A* consists of high-grade gneisses and amphibolites ($\sim 700^\circ\text{C}/\sim 0.4\text{ GPa}$) that show similarities to high-grade rocks of the Moldanubian domain. *Unit B* comprises kyanite–garnet mica schists and quartzites ($670^\circ\text{--}630^\circ\text{C}/\sim 0.9\text{ GPa}$) that are chemically similar to the metaclastics of the Villé unit in the Vosges (Müller, 1989). *Unit C* is represented by low-grade metasediments and metavolcanics ($400^\circ\text{--}450^\circ\text{C}/\sim 0.2\text{ GPa}$). Rare fossils point

to a late Silurian age of this unit (Mehl, 1988). Post-accretionary intrusion of a hornblende–biotite granite into the low-grade metamorphics of unit C caused contact metamorphism reaching temperatures of 520°–620°C at the contact (Wickert et al., 1990).

2.2. Intrusive rock units and age constraints

On the basis of intrusive relations and mineralogical and geochemical arguments, the plutonic rocks from the northern Vosges can be classified into five suites (see also von Eller, 1964, 1965, 1968, 1969; von Eller et al., 1970, 1971a,b; de Béthune et al., 1968; de la Roche and von Eller, 1969; Hahn-Weinheimer et al., 1971; Leterrier, 1978): (1) Early Carboniferous plutonic activity started with the intrusion of mafic magmas resulting in a more or less continuous band of *diorite* in the south (Neuntelstein unit) and isolated dioritic plugs in the north (Muckenbach unit) (Fig. 1c). (2) In the south of the ‘Bande médiane’ (a more or less continuous zone of early Carboniferous calc-alkaline volcanics), the granodioritic units of Hohwald South, Hohwald North and Champ-du-Feu South build up the *Southern Suite* (SS). (3) In the north of the ‘Bande médiane’, the I-type granitic intrusions of Champ-du-Feu North, Waldersbach (also known as ‘Granite de la Serva’) and Fouday form the *Northern Suite* (NS). (4) The *younger I-type granites* (YG) of Andlau, Natzwiller and Senones were intrusively emplaced into the older plutonic rocks, the late Devonian to early Carboniferous volcano-sedimentary sequences and/or the schists of Steige and Villé (Fig. 1c). (5) *Peraluminous alkalic S-type granites* and subvolcanic intru-

sions (Kagenfels, Kreuzweg, Grendelbruch) cross-cut the older plutonic rocks and their contact aureoles.

In the northern Schwarzwald (Fig. 1d), intrusion of the biotite–hornblende granite of Baden–Baden followed the accretion of tectonic units A to C along the dextral shear zone of Baden–Baden. Petrographic characteristics of the Baden–Baden granite are similar to those of the YG from the northern Vosges.

Reliable ages for the various intrusive suites are sparse. For the oldest intrusions, the diorites, Edel et al. (1986) and Boutin et al. (1995) reported conventional K–Ar ages of 331 ± 11 and 326 ± 11 Ma ($\pm 2 \sigma$) on hornblende (Neuntelstein) and a mixture of hornblende and biotite (Muckenbach), respectively. We obtained a conventional K–Ar age of 326 ± 5 Ma and a $^{40}\text{Ar}/^{39}\text{Ar}$ total fusion age of 331.0 ± 3.0 Ma on hornblende from the Neuntelstein diorite (Table 1). Most of the published K–Ar data on biotite and hornblende from the SS and the NS are affected by high amounts of chlorite documented by low abundances of K (Edel et al., 1986; Boutin et al., 1995). These data scatter between about 336 and 297 Ma and do not permit a precise estimate of intrusion ages. Boutin et al. (1995) report a $^{40}\text{Ar}/^{39}\text{Ar}$ total fusion age of 325 ± 12 Ma ($\pm 2 \sigma$) and a plateau age of 331 ± 12 Ma on hornblende from the Hohwald South granodiorite (SS). For hornblende from the Champ-du-Feu South granodiorite (SS), we obtained K–Ar and $^{40}\text{Ar}/^{39}\text{Ar}$ total fusion ages of 328 ± 6 and 330.5 ± 3.0 Ma, respectively (Table 1). For a mineral separate from a dioritic enclave in the Waldersbach granite (NS) that consisted of about 90% hornblende and 10% intergrown biotite, we

Table 1

K contents and age results of the conventional and the $^{40}\text{Ar}/^{39}\text{Ar}$ total fusion measurements on hornblende (hbl) and biotite (bt) from northern Vosges granitoids ($\pm 2 \sigma$ errors)

Sample	Intrusive unit	Mineral	K [wt.%]	K–Ar age [Ma]	$^{40}\text{Ar}/^{39}\text{Ar}$ age [Ma]
A-1	Andlau (YG)	bt	5.74	328 ± 4	–
NW-128	Natzwiller (YG)	bt	6.01	330 ± 4	–
S-76	Senones (YG)	hbl	0.544	325 ± 4	328.0 ± 4.0
W-38	Waldersbach (NS)	bt	6.12	335 ± 4	–
W-42E	Waldersbach (NS)	hbl ^a	1.497	329 ± 4	329.0 ± 4.0
CFS-102	Champ-du-Feu S (SS)	hbl	0.408	328 ± 6	330.5 ± 3.0
N-4	Neuntelstein (diorite)	hbl	0.592	326 ± 5	331.0 ± 3.0

^aThis concentrate contains around 10 wt.% of intergrown biotite.

obtained K–Ar and $^{40}\text{Ar}/^{39}\text{Ar}$ total fusion ages of 329 ± 4 Ma. Biotite from the Waldersbach granite itself yielded a K–Ar age of 335 ± 4 Ma (Table 1).

For biotite from the Natzwiller granite (YG), Faul and Jäger (1963) published K–Ar and Rb–Sr ages of 332 and 338 Ma, respectively (recalculated with new constants). A relatively high K–Ar age of 351 ± 12 Ma on biotite was given by Edel et al. (1986) and Boutin et al. (1995). The same biotite yielded a $^{40}\text{Ar}/^{39}\text{Ar}$ total fusion age of 336 ± 1 Ma and a ‘plateau age’ of 340.4 ± 1.2 Ma (Boutin et al., 1995). We obtained a conventional K–Ar age of 330 ± 4 Ma on a biotite concentrate (\pm chlorite) (Table 1). A hornblende sample from the Senones granite (YG) yielded K–Ar and $^{40}\text{Ar}/^{39}\text{Ar}$ ages of 325 ± 4 and 328 ± 4 Ma, respectively. Published ages for biotite from the Andlau granite (YG) are not reliable due to low K contents (Edel et al., 1986; Boutin et al., 1995). One biotite sample including minor amounts of chlorite yielded a K–Ar age of 328 ± 4 Ma (Table 1).

The emplacement age of the Kagenfels S-type granite has been constrained at 331 ± 5 Ma by Hess et al. (1995) on the basis of conventional K–Ar and $^{40}\text{Ar}/^{39}\text{Ar}$ total fusion data on biotite as well as single zircon radiogenic $^{207}\text{Pb}/^{206}\text{Pb}$ ratios. This age is corroborated by a $^{40}\text{Ar}/^{39}\text{Ar}$ total fusion age of 329 ± 2 Ma on biotite published by Boutin et al. (1995). In conclusion, we suggest that intrusive emplacement of all the granitoids from the northern Vosges took place within a limited time interval between about 336 and 330 Ma.

3. Analytical techniques

Major elements and the trace elements Rb, Ba, Th, Nb, Sr, Zr, Y, Cr and Ni were determined by wavelength dispersive X-ray fluorescence spectrometry (XRF) using standard techniques. For further details, see Altherr et al. (1995). The trace elements Cs, Th, U, Ta, Hf and Sc and the rare earth elements (REE) of selected samples (3–5 kg) were determined by instrumental neutron activation analysis (INAA) at Karlsruhe University. For details, see Class et al. (1994). For the determination of ferrous iron about 500 mg sample powder were decomposed in a platinum crucible by adding HF/HSO_4 . Crucible and

sample were then submerged into a boric acid solution and the ferrous iron liberated was titrated using potassium permanganate as an indicator. H_2O was determined by the Karl–Fischer titration method. CO_2 was analyzed by IR gas absorption spectrometry after inductive heating and combustion of the sample in an oxygen atmosphere.

For determination of Sr and Sm–Nd isotope ratios sample powders were decomposed in $\text{HF}-\text{HClO}_4$ in teflon bombs at 180°C for one week. Sr, Sm and Nd were separated by conventional ion exchange techniques and analyzed on single W and Re double filaments, respectively. Total procedure blanks are < 100 pg for Sr and < 50 pg for Sm and Nd, and they are negligible for the samples of this study. A detailed description of the analytical procedures is given by Hegner et al. (1995). Isotope ratios were measured on a Finnigan-MAT 262 multicollector mass spectrometer employing a static mode for Sr and Sm and a dynamic multiple mass collection routine for Nd. Sr isotope ratios are normalized to $^{86}\text{Sr}/^{88}\text{Sr} = 0.1194$. During the course of this study, four analyses of NBS 987 gave $^{87}\text{Sr}/^{86}\text{Sr} = 0.710218 \pm 17$ (1 s.d.), and two analyses of BCR-1 gave $^{87}\text{Sr}/^{86}\text{Sr} = 0.704972 \pm 10$ (1 s.d.). Within-run errors (2 σ mean) are less than 0.000015 and external precision (2 σ of population) is estimated to 0.00002. XRF data with 95% confidence limits of $\pm 3\%$ were used to calculate $^{87}\text{Rb}/^{86}\text{Sr}$ ratios. Nd isotope ratios are normalized to $^{146}\text{Nd}/^{144}\text{Nd} = 0.7219$. Measurements of the La Jolla standard provided a mean value of $^{143}\text{Nd}/^{144}\text{Nd} = 0.511855 \pm 5$ (1 s.d.; $n = 6$). Furthermore, two analyses of the BCR-1 reference material yielded $^{143}\text{Nd}/^{144}\text{Nd} = 0.512634 \pm 9$ (1 s.d.), 6.58 ppm Sm, 28.82 ppm Nd and $^{147}\text{Sm}/^{144}\text{Nd} = 0.1382$. Within-run errors on $^{143}\text{Nd}/^{144}\text{Nd}$ ratios are < 0.00001 and the external precision is estimated to be better than 0.000015 at the 95% confidence level.

4. Results

4.1. Rock textures and modal compositions

Apart from local shear zones and pseudotachylite veins all the granitoids including mafic microgranular enclaves display isotropic igneous textures. Mi-

crodiioritic enclaves from the Waldersbach granite (NS) have diameters up to a few meters and are characterized by fine-grained rims and acicular hornblende and apatite grains as well as thin platy biotite crystals ('Nadeldiorit'; von Eller, 1965). Such textures suggest rapid cooling ('quenching') in a colder granite host magma. In the Hohwald South granodiorite (SS), larger feldspar grains may occur along the boundary between enclaves (diameters up to 30 cm)

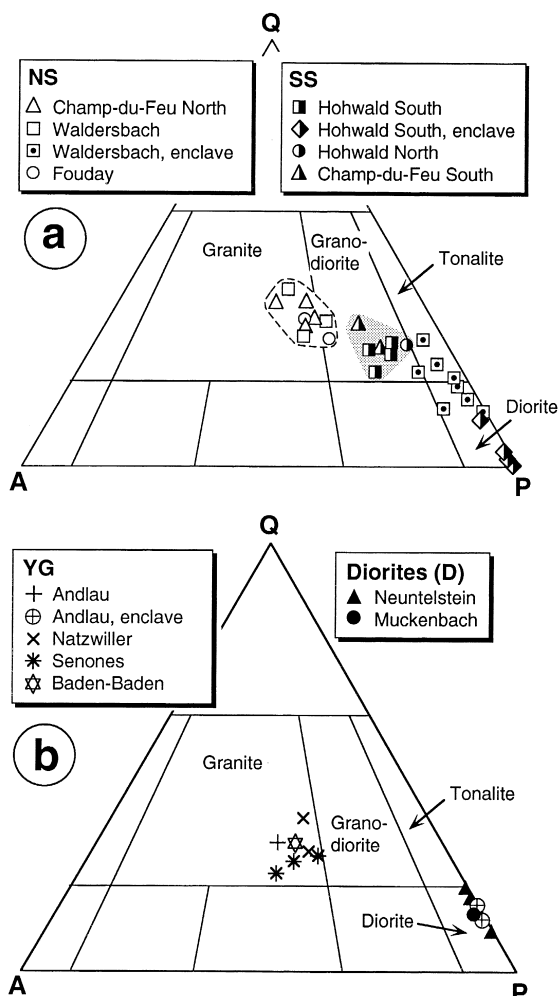


Fig. 2. Modal compositions of representative I-type granitoid samples from the northern Vosges and Schwarzwald in terms of quartz (Q), alkali feldspar (A) and plagioclase (P). Nomenclature taken from Streckeisen (1976). (a) Samples from the northern (NS) and southern (SS) intrusive suites; (b) samples from the diorites (D) and YG.

Table 2

Pressure estimates for granitoids from the northern Vosges obtained from Al-in-hornblende barometry ($\pm 1 \sigma$ errors)

Sample	Rock type	Pressure [GPa]
<i>Diorites from Neuntelstein and Muckenbach</i>		
N-4	biotite–hornblende diorite	0.33 ± 0.04
N-79	biotite–hornblende diorite	0.35 ± 0.03
M-52	biotite–hornblende diorite	0.14 ± 0.08
<i>Southern Granodioritic Suite (SS)</i>		
HS-25	biotite–hornblende granodiorite	0.23 ± 0.06
HS-27E	hornblende diorite, enclave	0.22 ± 0.03
HN-86	biotite–hornblende granodiorite	0.16 ± 0.04
CFS-102	biotite–hornblende granodiorite	0.17 ± 0.03
<i>Northern Granitic Suite (NS)</i>		
W-42E	biotite–hornblende diorite, enclave	0.19 ± 0.03
<i>Younger granites (YG)</i>		
A-24E	hornblende–biotite diorite, enclave	0.09 ± 0.02
NW-96	hornblende–biotite granite	0.10 ± 0.06
S-76	hornblende–biotite granite	0.12 ± 0.03

and host rock, indicating mingling of dioritic and granodioritic magmas.

Modal compositions in terms of quartz, alkali feldspar and plagioclase are plotted in Fig. 2. Among the older granitoids (OG), rocks from the SS display a restricted range of granodioritic compositions; microgranular enclaves from the Hohwald South unit are diorites (Fig. 2a). Rocks from the NS are transitional between granodiorite and granite. These rocks will be collectively referred to as granites in the following. The Waldersbach granite contains microgranular enclaves of dioritic to tonalitic compositions. Rocks from the Neuntelstein and Muckenbach units are always dioritic (Fig. 2b). As compared with the older granites from the NS, the YG from the Vosges and the Schwarzwald tend to have lower contents of quartz (Fig. 2b). Microgranular enclaves in the Andlau granite (YG) have dioritic compositions.

The *diorites* from Neuntelstein and Muckenbach consist of hornblende, biotite, plagioclase, minor amounts of quartz and titanite, apatite, magnetite, zircon and alkali feldspar as accessory phases. *Granodiorites from the SS* are all very similar and contain biotite, hornblende, magnetite, titanite, apatite, allanite and zircon, besides plagioclase, orthoclase and

quartz. *NS granites* display heterogenous textures ranging from more porphyric varieties (Waldersbach) to more equigranular types (Champ-du-Feu

North, Fouday). Besides plagioclase, perthitic orthoclase and quartz, these granites contain biotite, titanite, allanite, apatite, zircon and magnetite. The Fou-

Table 3

Major [wt.%] and trace element [ppm] abundances in representative samples from the different intrusive rock suites. OG, northern Vosges: Neuntelstein dioritic suite (N), Muckenbach diorites (M), Hohwald South (HS), Hohwald North (HN), Champ-du-Feu South (CFS), Champ-du-Feu North (CFN), Waldersbach (W), Fouday (F). YG: Andlau (A), Natzwiller (NW), Senones (S), Baden–Baden, Schwarzwald (BB). Rock types: hornblende diorite (D), granodiorite (Gdr), granite (Gr). See text for analytical techniques

Intrusive unit	N	N	N	N	M	HS	HS	HN	CFS	CFN	W
Sample	3	4	13	79	52	25	27E	86	114	90	37
Rock type	Hbl-D	Hbl-D	Hbl-D	Hbl-D	Hbl-D	Gdr	Hbl-D	Gdr	Gdr	Gr	Gr
SiO ₂	52.47	53.29	61.96	52.09	55.11	64.78	55.29	65.43	64.44	72.40	73.16
TiO ₂	0.96	1.09	0.60	1.13	1.09	0.53	0.85	0.55	0.54	0.26	0.24
Al ₂ O ₃	16.72	18.15	17.80	18.43	18.95	16.38	17.78	16.67	15.88	14.07	13.79
Fe ₂ O ₃	2.22	2.90	1.77	3.50	1.73	1.79	2.51	2.12	2.23	0.74	0.70
FeO	6.23	5.81	3.00	5.52	4.79	2.61	4.80	2.20	2.50	1.66	1.45
MnO	0.15	0.19	0.12	0.20	0.15	0.10	0.23	0.11	0.12	0.08	0.06
MgO	6.91	4.05	1.46	4.36	2.78	1.87	4.19	1.71	2.44	0.51	0.50
CaO	7.76	6.98	4.30	7.02	7.21	4.39	5.92	4.49	2.53	1.44	1.25
Na ₂ O	2.29	3.24	3.89	2.55	3.28	3.62	3.91	3.55	3.34	3.46	2.96
K ₂ O	1.56	1.61	2.68	2.03	1.94	2.77	2.52	2.20	3.37	4.38	5.19
P ₂ O ₅	0.15	0.25	0.21	0.18	0.32	0.16	0.20	0.16	0.16	0.08	0.09
H ₂ O	2.04	1.85	1.34	2.56	2.09	0.94	1.65	1.08	1.76	0.83	0.69
Total	99.46	100.04	99.13	99.57	99.44	99.94	99.85	100.27	99.31	99.91	100.08
Mg#	62.5	48.8	38.7	49.9	46.5	46.7	54.0	45.2	51.7	30.3	32.3
Cr	n.a.	40	21	25	43	19	61	22	20	13	13
Ni	77	13	6	12	13	10	23	7	10	7	6
Sc	n.a.	27.7	n.a.	25.0	19.4	9.8	22.7	8.6	10.8	7.3	n.a.
Ga	18	22	22	21	20	19	21	18	18	17	15
Cs	n.a.	4.6	n.a.	12.5	5.3	2.8	6.5	5.1	11.1	4.9	n.a.
Rb	58	57	91	90	72	84	110	65	113	174	146
Sr	411	429	383	374	473	359	369	405	294	145	137
Ba	404	418	681	500	476	536	553	552	634	698	747
Zr	86	81	254	111	112	112	144	127	118	162	154
Hf	n.a.	2.17	n.a.	2.95	2.87	3.35	4.13	4.12	3.70	4.73	n.a.
Nb	6	8	11	9	9	9	14	8	10	12	9
Ta	n.a.	0.36	n.a.	0.52	0.50	0.59	0.78	0.52	0.77	0.85	n.a.
Th	3.0	5.4	12.0	5.3	5.6	10.1	8.2	9.3	10.5	11.9	12.0
U	n.a.	1.4	n.a.	2.1	1.4	2.5	2.1	2.5	3.0	3.9	n.a.
Y	22	33	31	30	27	19	36	17	25	27	26
Pb	17	20	19	50	19	20	17	20	14	28	26
Zn	105	118	72	103	91	54	97	56	65	42	34
La	n.a.	24.0	n.a.	22.3	25.5	28.2	23.9	33.6	28.2	39.8	n.a.
Ce	n.a.	44.9	n.a.	42.9	46.4	48.0	50.4	51.0	47.3	63.1	n.a.
Nd	n.a.	28.3	n.a.	25.0	28.0	24.1	28.2	23.1	24.2	30.9	n.a.
Sm	n.a.	5.87	n.a.	5.45	5.45	4.31	6.76	3.78	4.66	5.29	n.a.
Eu	n.a.	1.48	n.a.	1.35	1.60	1.05	1.51	1.07	1.07	0.80	n.a.
Gd	n.a.	6.0	n.a.	5.9	5.5	4.5	5.8	3.7	4.6	5.2	n.a.
Tb	n.a.	1.01	n.a.	1.01	0.92	0.67	0.91	0.61	0.84	0.80	n.a.
Ho	n.a.	1.17	n.a.	1.07	0.93	0.72	1.10	0.68	0.86	0.88	n.a.
Tm	n.a.	0.40	n.a.	0.41	0.40	0.30	0.54	0.29	0.38	0.41	n.a.
Yb	n.a.	2.69	n.a.	2.72	2.15	1.74	3.43	1.57	2.34	2.67	n.a.
Lu	n.a.	0.42	n.a.	0.42	0.34	0.29	0.51	0.27	0.34	0.39	n.a.

day granite locally contains small amounts of hornblende. The YG tend to have porphyritic textures with larger orthoclase crystals in a medium-grained

matrix consisting of plagioclase, orthoclase, quartz, biotite and small amounts of hornblende, titanite, apatite, allanite, zircon and magnetite.

Intrusive unit	W	W	W	W	F	A	A	NW	NW	S	BB
Sample	38	47	36E	42E	59	1	24E	96	127	76	200
Rock type	Gr	Gr	T	Hbl-D	Gr	Gr	Hbl-D	Gr	Gr	Gr	Gr
SiO ₂	69.73	73.39	66.73	59.12	69.97	70.70	58.29	68.54	73.51	66.51	68.10
TiO ₂	0.36	0.24	0.49	0.79	0.32	0.38	0.93	0.50	0.35	0.67	0.44
Al ₂ O ₃	15.17	13.89	15.98	17.17	14.95	14.84	17.05	14.87	13.36	14.68	15.97
Fe ₂ O ₃	0.73	0.29	0.95	2.07	1.00	1.14	2.80	1.37	1.09	1.68	1.16
FeO	2.26	1.78	3.15	4.49	1.73	1.48	4.06	1.43	0.93	1.71	1.30
MnO	0.13	0.05	0.10	0.22	0.07	0.08	0.26	0.06	0.02	0.06	0.05
MgO	0.79	0.52	1.60	2.47	0.66	0.93	3.29	1.41	1.08	2.24	1.26
CaO	2.22	1.89	2.72	5.40	2.19	2.45	4.94	1.87	0.94	2.55	2.16
Na ₂ O	3.64	3.21	4.13	3.74	4.01	3.48	3.81	3.49	3.12	3.73	4.54
K ₂ O	3.83	4.47	2.77	2.65	3.92	4.11	2.28	4.91	4.97	4.79	4.19
P ₂ O ₅	0.14	0.08	0.20	0.22	0.11	0.13	0.23	0.21	0.21	0.26	0.21
H ₂ O	0.90	0.54	0.96	1.37	0.56	0.65	1.28	0.59	0.58	0.74	0.79
Total	99.90	100.34	99.78	99.71	99.49	100.37	99.22	99.25	100.16	99.62	100.17
Mg#	34.9	33.5	44.2	43.5	33.2	42.4	49.8	51.2	52.8	57.9	51.6
Cr	10	24	17	14	16	13	40	26	26	53	16
Ni	6	5	7	5	7	6	15	18	17	32	7
Sc	6.4	n.a.	n.a.	15.9	7.2	6.5	n.a.	4.7	n.a.	6.3	4.3
Ga	18	15	20	20	19	17	23	22	22	21	24
Cs	5.0	n.a.	n.a.	8.1	4.6	5.3	n.a.	4.1	n.a.	5.6	4.1
Rb	154	136	144	126	157	175	212	191	253	194	139
Sr	194	176	218	334	196	275	380	672	333	585	689
Ba	629	882	437	475	836	872	557	1092	510	1052	1700
Zr	153	114	180	132	189	135	146	186	143	190	200
Hf	4.79	n.a.	n.a.	3.62	4.92	3.96	n.a.	6.21	n.a.	6.48	6.39
Nb	11	8	15	10	12	13	12	26	25	23	13
Ta	0.80	n.a.	n.a.	0.71	0.75	1.15	n.a.	1.66	n.a.	1.73	0.90
Th	13.8	11.0	14.0	7.1	12.7	15.9	6.0	33.8	44.0	32.8	23.3
U	4.9	n.a.	n.a.	2.9	4.1	4.2	n.a.	8.3	n.a.	7.4	4.4
Y	32	19	40	37	32	23	35	19	12	18	11
Pb	33	35	16	15	35	29	12	66	30	27	34
Zn	57	32	60	107	53	36	106	43	26	43	45
La	35.0	n.a.	n.a.	24.3	39.3	35.9	n.a.	86.2	n.a.	71.8	52.5
Ce	57.2	n.a.	n.a.	48.6	68.3	58.1	n.a.	131.0	n.a.	114.0	92.9
Nd	27.1	n.a.	n.a.	30.0	33.1	26.5	n.a.	56.0	n.a.	50.5	32.6
Sm	5.49	n.a.	n.a.	5.91	6.02	4.75	n.a.	7.87	n.a.	7.27	5.59
Eu	0.84	n.a.	n.a.	1.33	1.11	0.93	n.a.	1.46	n.a.	1.44	1.28
Gd	6.2	n.a.	n.a.	7.0	6.8	4.6	n.a.	7.8	n.a.	6.5	3.5
Tb	0.98	n.a.	n.a.	1.19	1.02	0.73	n.a.	0.89	n.a.	0.85	0.45
Ho	1.13	n.a.	n.a.	1.30	1.14	0.81	n.a.	0.74	n.a.	0.65	n.a.
Tm	0.49	n.a.	n.a.	0.61	0.43	0.34	n.a.	0.27	n.a.	0.27	0.17
Yb	2.90	n.a.	n.a.	3.74	2.87	2.01	n.a.	1.46	n.a.	1.46	0.96
Lu	0.45	n.a.	n.a.	0.55	0.44	0.32	n.a.	0.26	n.a.	0.25	0.17

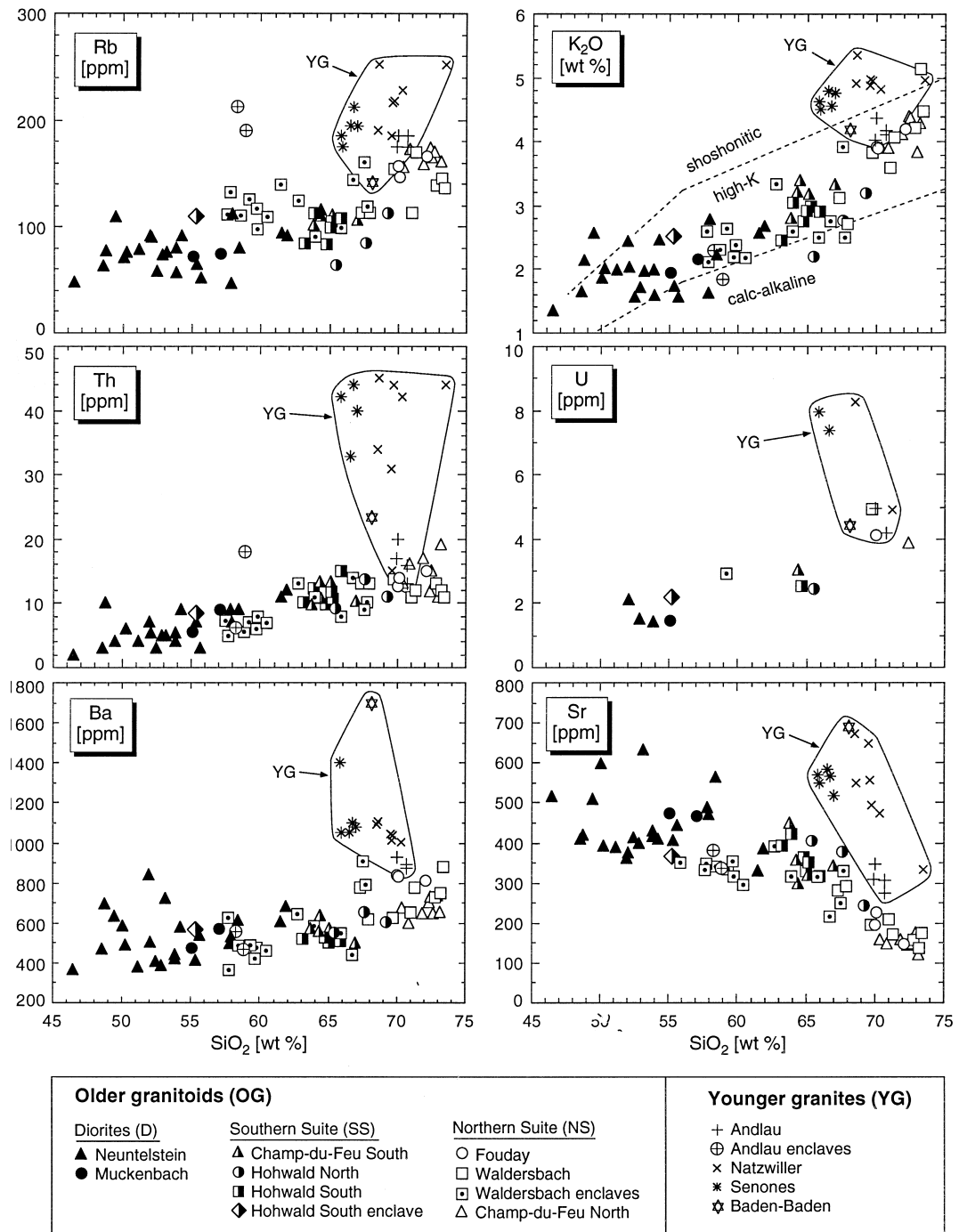


Fig. 3. Selected Harker variation diagrams for I-type granitoids from the northern Vosges and Schwarzwald illustrating some of the chemical contrasts that distinguish the different intrusive rock suites. Note that for similar SiO_2 , the YG tend to have higher abundances of large ion lithophile elements (Rb, K, Th, U, Ba, Sr), La, Nb and P, but lower abundances of Yb and Sc than the older NS and SS granitoids. Granodiorites from the SS have significantly lower abundances of Zr than granites from the NS.

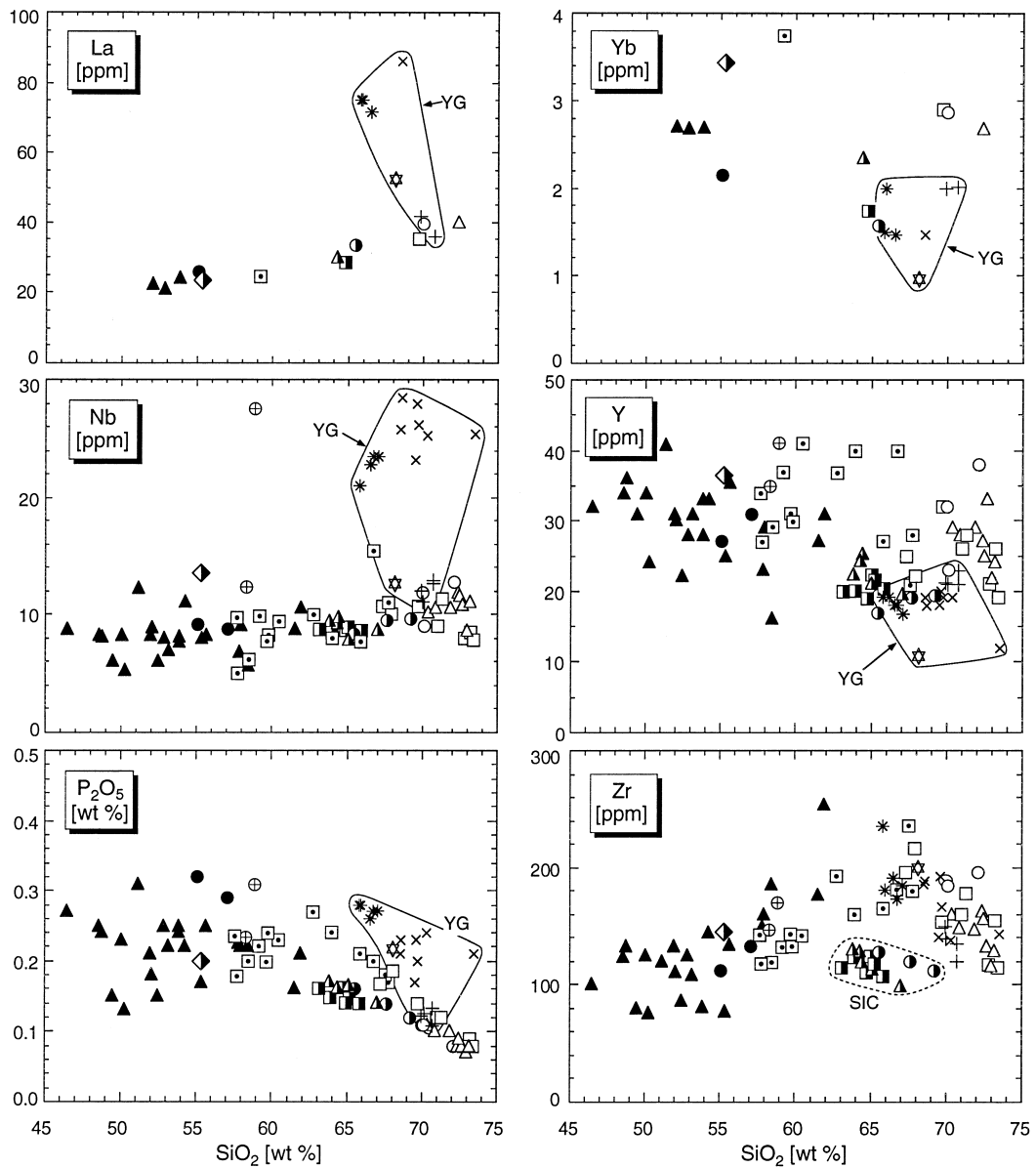


Fig. 3 (continued).

4.2. Depth of intrusion

Some of the granitoids from the northern Vosges contain the critical mineral assemblage hornblende + biotite + plagioclase + alkali feldspar + quartz + titanite + titanomagnetite + apatite that (together with melt) is required for application of the Al-hornblende barometer (Schmidt, 1992). For our pressure estimates, we used rim compositions of hornblende grains in contact with quartz and alkali feldspar. Cation calculations were based on 23 oxygens and a cation number of 13 excluding Ca, Na and K. Pressure values (Table 2) tend to decrease in the order of decreasing intrusion age, i.e., from the

Neuntelstein diorite via the SS granodiorites and NS granites to the YG. Whereas the pressure of about 0.34 GPa, deduced for the intrusion and final crystallization of the Neuntelstein diorite, corresponds to a depth of about 10 km, the YG solidified at significantly shallower depths of about 3 km. A greater intrusion depth of the Neuntelstein diorite as compared to the other plutonic rock units is further suggested by the occurrence of pseudotachylite veins at the type locality Neuntelstein.

4.3. Whole-rock chemistry

In the course of this study, a total of 94 fresh granitoid samples from the different intrusive units

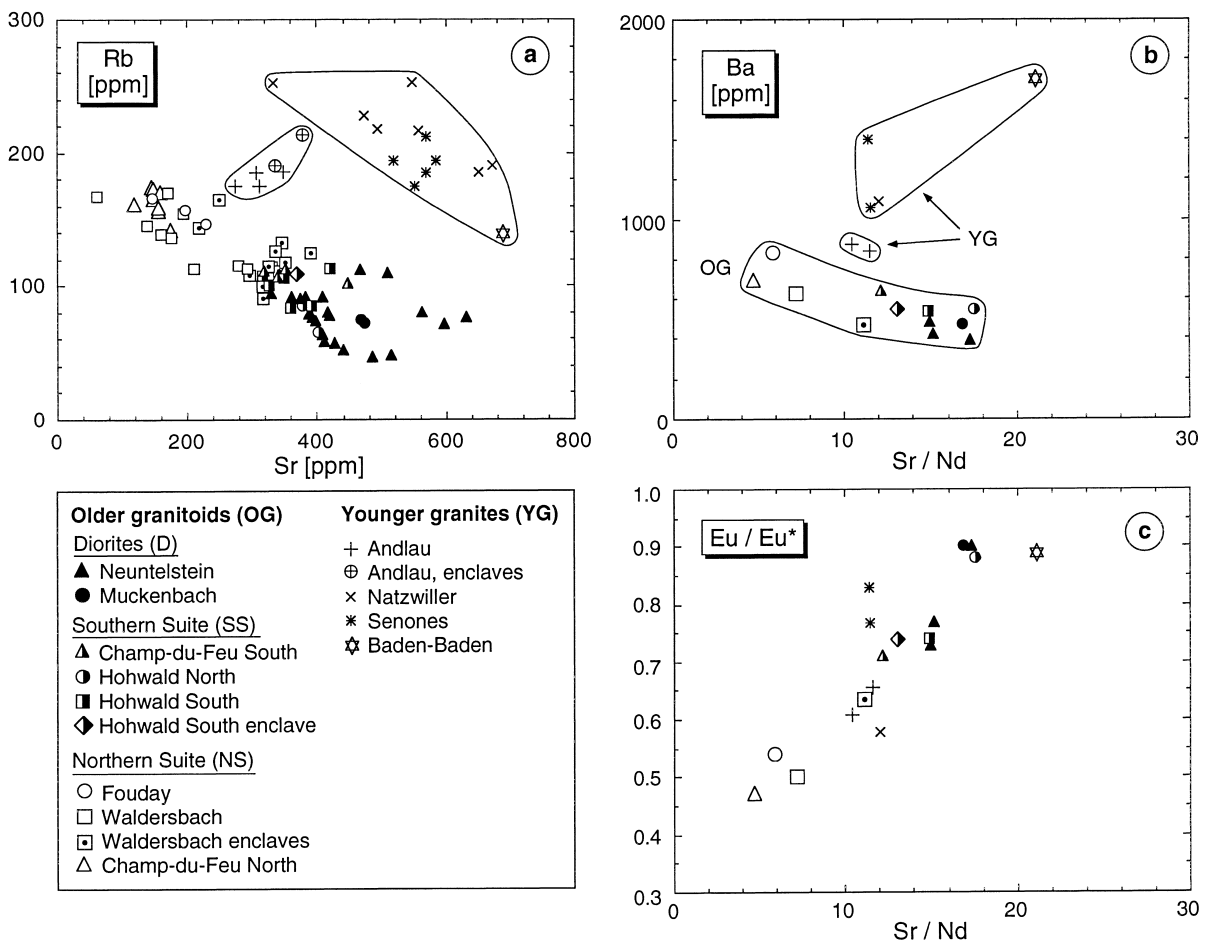


Fig. 4. Variation of some trace elements in granitoids from the northern Vosges and Schwarzwald. (a) Rb vs. Sr relationship. Note that YG samples plot to the high-Rb/high-Sr side of the trend defined by the OG. (b) Ba vs. Sr/Nd diagram displaying higher abundances of Ba in the YG as compared with the OG. (c) Covariation of Eu/Eu^* [$= \text{Eu}_{\text{cn}} \times (\text{Sm}_{\text{cn}} \times \text{Gd}_{\text{cn}})^{-0.5}$; cn = chondrite-normalized] and Sr/Nd ratios suggesting fractionation of plagioclase as a major cause of the negative Eu anomalies.

were collected for analysis. Twenty-two selected chemical analyses of representative samples are given in Table 3. In addition, samples from the Neuntel-

stein diorite and the Andlau and Senones granites represent the international geochemical reference samples DR-N, GA and GS-N. Proposed values for

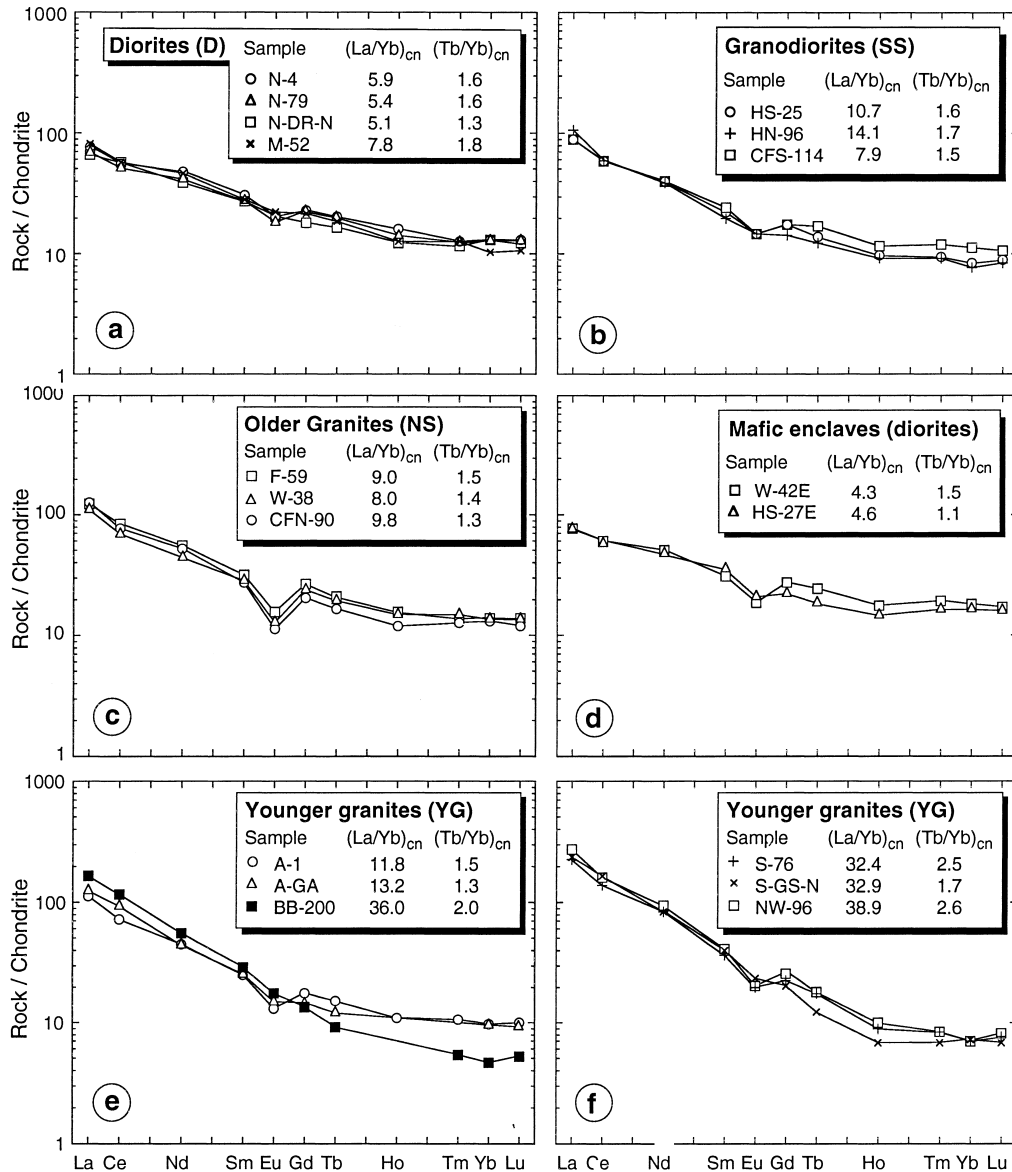


Fig. 5. (a–f) Chondrite-normalized REE abundance patterns (normalized to values given by Boynton, 1984) for representative samples from the northern Vosges and Schwarzwald. (a) Diorites from Neuntelstein (N) and Muckenbach (M); (b) granodiorites from the southern Granodioritic Suite (SS): Hohwald South (HS), Hohwald North (HN) and Champ-du-Feu South (CFS); (c) granites from the northern Granitic Suite (NS): Champ-du-Feu North (CFN), Waldersbach (W) and Fouday (F); (d) mafic enclaves (diorites) from the HS granodiorite and W granite; (e) YG from Andlau (A) and Baden–Baden (BB); (f) YG from Senones (S) and Natzwiller (NW). Values for samples N-DR-N, A-GA and S-GS-N were taken from Govindaraju and Roelandts (1989), Bedard and Barnes (1990), Watkins and Nolan (1990), Verma (1991), Garbe-Schönberg (1993) and Reddy and Pant (1993).

these samples (Govindaraju and Roelandts, 1989; Bedard and Barnes, 1990; Watkins and Nolan, 1990; Verma, 1991; Verma et al., 1992; Garbe-Schönberg, 1993; Reddy and Pant, 1993) have been included in this study (e.g., REE data for some samples; Fig. 5).

The samples span a range of SiO₂ from about 46 to 74 wt.%, including diorites, dioritic to tonalitic mafic enclaves, granodiorites and granites (Fig. 3a and b). All samples are calc-alkaline (alkali–lime index ~ 60). The aluminium saturation index [ASI = molecular Al₂O₃/(CaO + K₂O + Na₂O)] increases with SiO₂ from about 0.80 to 1.15 (not shown) with all but five samples being characterized by ASI < 1.10. Samples from the OG units (diorites, SS granodiorites, NS granites) exhibit poorly defined data trends. As compared with the older granites of the NS, the YG tend to have higher contents of Rb, K, Th, U, Ba, Sr (Fig. 3a), La, Nb and P (Fig. 3b), but lower abundances of Yb and Y (Fig. 3b) at similar SiO₂.

Using the K₂O vs. SiO₂ nomenclature of Peccerillo and Taylor (1976), the OG classify as high-K calc-alkaline rocks with transitions to both normal calc-alkaline and shoshonitic suites (Fig. 3a). Samples from the YG plot near to or within the shoshonitic field.

The various rock suites are most readily distinguished by means of a Rb vs. Sr diagram (Fig. 4a). The OG form a continuous trend from high-Sr/low-Rb diorites via granodiorites (SS) to low-Sr/high-Rb granites (NS). The YG samples plot to the high-Rb/high-Sr side of this trend, whereby the Andlau granite plots at an intermediate position between the OG and the other YG. In a Ba vs. Sr/Nd diagram (Fig. 4b), the YG samples plot to the high-Ba side of the trend defined by samples from the OG. The systematic nature of the observed intra- and inter-suite variations in the abundances of Rb, Sr and Ba argues against significant post emplacement element mobility.

Chondrite-normalized (cn) REE patterns have concave-upward shapes which are most pronounced in some of the YG samples (Fig. 5). Among the OG from the northern Vosges, there is a systematic increase in both (La/Yb)_{cn} and (Tb/Yb)_{cn} ratios from the diorites via SS granodiorites to the NS granites (i.e., with increasing SiO₂) and the magnitude of the negative Eu anomalies [Eu/Eu* = Eu_{cn} × (Sm_{cn} × Gd_{cn})^{-0.5}] is most pronounced in the NS granites (Fig. 5a–d). As compared with the older NS granites, the YG show higher (La/Yb)_{cn} and (Tb/Yb)_{cn} ratios and less pronounced negative Eu

Table 4

Sm–Nd and Rb–Sr isotope data for granitoids from the northern Vosges and Schwarzwald. ⁸⁷Rb/⁸⁶Sr values were calculated from XRF data. Initial ϵ_{Nd} values [$\epsilon_{\text{Nd}}(\text{I})$] and initial Sr isotope ratios [⁸⁷Sr/⁸⁶Sr(I)] are based on 340 Ma. For errors, see Section 3

Sample	Sm	Nd	¹⁴⁷ Sm/ ¹⁴⁴ Nd	¹⁴³ Nd/ ¹⁴⁴ Nd	$\epsilon_{\text{Nd}}(\text{I})$	⁸⁷ Rb/ ⁸⁶ Sr	⁸⁷ Sr/ ⁸⁶ Sr	⁸⁷ Sr/ ⁸⁶ Sr(I)
<i>Diorites (D)</i>								
N-4	6.28	27.33	0.1390	0.512422	–1.7	0.57	0.707420	0.70466
N-79	5.66	25.64	0.1334	0.512353	–2.8	0.70	0.708803	0.70542
M-52	6.04	28.69	0.1272	0.512394	–1.7	0.47	0.708329	0.70605
<i>Granodiorites (SS)</i>								
HS-25	4.69	26.29	0.1078	0.512431	–0.2	0.69	0.708551	0.70521
HN-86	4.39	27.36	0.0969	0.512444	+0.5	0.47	0.707551	0.70528
CFS-114	4.95	25.66	0.1165	0.512439	–0.4	1.15	0.710694	0.70513
<i>Older Granites (NS)</i>								
CFN-90	7.17	40.58	0.1068	0.512311	–2.5	3.55	0.722029	0.70485
W-38	8.52	53.24	0.0968	0.512324	–1.8	2.31	0.716937	0.70576
F-59	6.91	35.44	0.1179	0.512343	–2.3	2.36	0.716887	0.70547
<i>Younger granites (YG)</i>								
A-1	5.38	31.19	0.1042	0.512265	–3.4	1.84	0.714222	0.70558
N-96	9.20	68.42	0.0813	0.512257	–2.6	1.15	0.709969	0.70457
S-76	10.60	70.98	0.0902	0.512310	–1.9	0.98	0.710585	0.70598
BB-200	6.53	46.95	0.0841	0.512311	–1.5	0.58	0.708657	0.70585

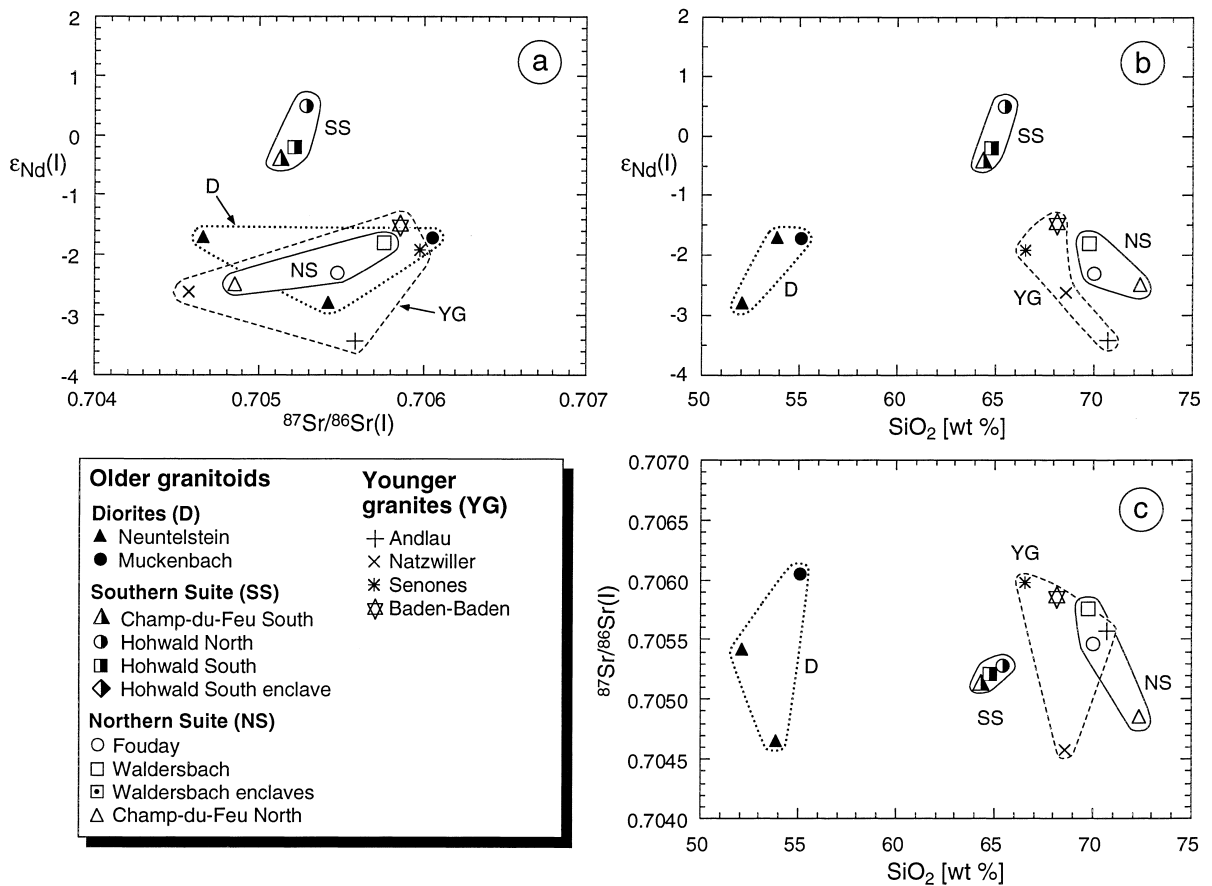


Fig. 6. (a–c) Variation diagrams showing isotopic compositions of selected samples from the different intrusive rock suites. (a) Initial ε_{Nd} value [$\varepsilon_{\text{Nd}}(\text{I})$] vs. initial Sr isotope ratio [$^{87}\text{Sr}/^{86}\text{Sr}(\text{I})$]; (b) bulk-rock $\varepsilon_{\text{Nd}}(\text{I})$ vs. SiO_2 ; (c) bulk-rock $^{87}\text{Sr}/^{86}\text{Sr}(\text{I})$ vs. SiO_2 .

anomalies (Fig. 5c, e and f). Eu/Eu^* values are correlated with Sr/Nd (Fig. 4c).

4.4. Nd–Sr isotope ratios

Thirteen bulk-rock Nd and Sr isotope data are listed in Table 4. Fig. 6a shows that there is no systematic variation of initial ε_{Nd} values [$\varepsilon_{\text{Nd}}(\text{I})$] with initial $^{87}\text{Sr}/^{86}\text{Sr}$ isotope ratios [$^{87}\text{Sr}/^{86}\text{Sr}(\text{I})$]. Neither $\varepsilon_{\text{Nd}}(\text{I})$ nor $^{87}\text{Sr}/^{86}\text{Sr}(\text{I})$ values show a systematic variation with bulk rock composition (e.g., SiO_2 ; Fig. 6b and c). Whereas the diorites, the older granites from the NS and the YG show similar ranges of $\varepsilon_{\text{Nd}}(\text{I})$ and $^{87}\text{Sr}/^{86}\text{Sr}(\text{I})$, the granodiorites

from the SS are characterized by significantly higher $\varepsilon_{\text{Nd}}(\text{I})$ values.

Since the isotopic characteristics of most micro-granular enclaves are usually not representative of their primary mafic magmas but have been substantially modified by mass transfer between enclaves and hosts (e.g., Pin et al., 1990; Holden et al., 1991; Elburg, 1996) no attempt was made to determine the Sr–Nd isotopic signatures of the enclaves in the different granodioritic and granitic hosts.

Nd and Sr isotopic compositions of the I-type granitoids from the northern Vosges and northern Schwarzwald are within the range of values shown by the early Carboniferous granitoids from the tectonic units II and III in the Odenwald located in the northern part of the SZ (Altherr et al., 1999).

5. Discussion

5.1. Tectonic setting

Our present knowledge of the Central European Variscides does not allow for a detailed reconstruction of the plate tectonic setting in early Carboniferous time (e.g., Bachtadse et al., 1995; Franke et al., 1995; Oncken, 1997; Tait et al., 1997). In particular, there are rather poor constraints on the duration of southward-directed subduction beneath the Saxothuringian and Moldanubian domains (Armorica) and the final closure of the Rheohercynian ocean. The culmination of high-pressure/low-temperature metamorphism in the northern Phyllite Zone and the southern Rheohercynian Zone (Fig. 1) is only slightly older than 325 Ma (K–Ar on phengitic mica; Ahrendt et al., 1983; Massonne, 1995) and the formation of eclogites in the composite Moldanubian Schwarzwald has been dated at ~336 Ma by the Sm–Nd method (Kalt et al., 1994). In the autochthon of the Rheohercynian Zone (East Avalonia), syn-orogenic clastic sedimentation started not later than the early Carboniferous III α representing an upper time limit for the emplacement of allochthonous units derived from the northern part of Armorica and, hence, for the closure of the Rheohercynian ocean (Franke, 1995). Time constraints on the accretionary processes forming the complex Saxothuringian Zone are rather poor (Oncken, 1997). It is therefore not clear whether the end of accretion in the northern Vosges and Schwarzwald forming part of the southernmost Saxothuringian Zone is tantamount to the cessation of southward-directed subduction. Hence, the I-type granitoids of this study were generated either above an active subduction zone or in a syn to post-collisional setting. Trace element signatures of granitoid rocks do not allow for a discrimination between these settings, as they are strongly dependent on protolith composition (e.g., Roberts and Clemens, 1993; Pearce, 1996).

5.2. Intra-pluton and intra-suite evolution

For most elements the OG as a whole form poorly defined Harker trends whereby the diorites display the largest scatter and both the SS and the NS host rocks show limited compositional variation (Fig. 3).

The abundances of K, Rb, Th, U, Ba, La and Nb, for example, increase with increasing SiO₂, whereas those of Sr and P decrease. The OG rocks also form coherent fractionation trends in other element variation diagrams, such as Rb vs. Sr, Ba vs. Sr/Nd and Eu/Eu* vs. Sr/Nd (Fig. 4). The observed systematic chemical variation of the OG from diorites via granodiorites (SS) to granites (NS) could readily be explained by increasing fractionation of plagioclase and biotite, accompanied by amphibole and accessory phases, such as sphene, apatite (at SiO₂ > 60 wt.%) and zircon (at SiO₂ > 65 wt.%). Such a fractionation trend is also suggested by the variation in modal compositions (Fig. 2) and REE patterns (Fig. 5). Fractionation of amphibole should increase La/Yb values of the residual melts and in more evolved systems the residual melts should develop cn REE patterns with a concave-upward shape (e.g., Romick et al., 1992) as shown by the SS and NS samples (Fig. 5b and c). A strictly comagmatic relationship of all OG rocks can be ruled out by their different initial radiogenic isotope compositions. While all OG rocks show similar ⁸⁷Sr/⁸⁶Sr(I) between about 0.7045 and 0.7061, the granodiorites of the SS have significantly higher $\epsilon_{\text{Nd}}(\text{I})$ values than the diorites and the NS granites (Fig. 6). Unless distinct contamination processes are envisaged, these differences in Nd isotopic signatures suggest that the three OG magma suites were derived from different sources.

Mafic microgranular enclaves of the Waldersbach granite (NS) and the Hohwald South granodiorite (SS) fit into the element variation trends defined by the bulk of the OG rocks (Figs. 3 and 4). The cn REE patterns of two microdioritic enclaves are similar to those of the diorites (compare Fig. 5a and d). Since microstructural evidence indicates an origin of the microgranular enclaves by mingling and mixing of mafic and more felsic magmas (see Section 4.1), we conclude that dioritic magmas were continuously intruded before and during the emplacement of the granodioritic and granitic magma pulses forming the SS and NS.

As compared with the older granites of the NS, the YG rocks are characterized by higher abundances of LILE, La, Nb and P, but lower contents of Y and HREE (Fig. 3bFig. 5). These plutons also show different trends in other element variation diagrams

such as Rb vs. Sr or Ba vs. Sr/Nd (Fig. 4) and they have higher Eu/Eu* (Figs. 4 and 5). Their radiogenic isotope compositions are, however, similar to those of the diorites and the NS granites (Fig. 6).

5.3. Genesis of dioritic units

The diorites represent the oldest magma pulses in the northern Vosges. The size of the intrusive bodies is too large to allow for a substantial modification of their chemical and isotopic characteristics by the younger more felsic magma pulses forming the SS and NS. Therefore, the chemical and isotopic signatures of these rocks have to be regarded as primary features reflecting source composition, melting conditions and fractionation. High abundances of incompatible elements (Fig. 3a and b) in combination with an enriched isotopic signature, i.e., low $\epsilon_{\text{Nd}}(\text{I})$ (–1.7 to –2.8) and relatively high $^{87}\text{Sr}/^{86}\text{Sr}(\text{I})$ values (0.7046–0.7061), suggest either an enriched lithospheric mantle source or derivation by very large degrees of partial melting of alkaline mafic crustal rocks.

Several experimental studies (e.g., Wolf and Wyllie, 1994; Rapp, 1995; Rapp and Watson, 1995; and references therein) have shown that extremely high temperatures in excess of $\sim 1100^\circ\text{C}$ are required to produce mafic metaluminous low-silica (< 58 wt.%) melts by dehydration melting of metabasaltic compositions. Regardless of the degree of partial melting, such melts are generally characterized by low Mg\# [$= \text{molar } 100 \times \text{MgO}/(\text{MgO} + 0.9\text{FeO}_{\text{tot}})$] (< 44.0) and high contents of Na_2O (> 4.3 wt.%), i.e., features that are not shown by the diorites from the Vosges (Table 3; Fig. 7a). Mafic melt compositions coexist with granulite residues (clinopyroxene + plagioclase \pm orthopyroxene \pm olivine) below about 1.0 GPa and with garnet granulite or eclogite residues at higher pressures (Rapp and Watson, 1995). The diorites from the Vosges show nearly unfractionated HREE abundances (Fig. 5) with low $(\text{La}/\text{Yb})_{\text{cn}}$ and $(\text{Tb}/\text{Yb})_{\text{cn}}$ values and they have high abundances of Y (Fig. 3b) and high ratios of Sr/Y (Fig. 7b). All these features preclude the involvement of substantial amounts of garnet either in the residue during partial melting and ‘final’ reequilibration, or as part of the fractionating assemblage in a deep crust. Generation of the dioritic magmas by partial melting

of mafic crustal source rocks would therefore imply that temperatures of more than about 1100°C were reached in a depth of less than about 33 km (corresponding to the appearance of garnet in mafic rock systems at pressures above 1.0 GPa; e.g., Rapp and Watson, 1995). Such high geothermal gradients have to be regarded as highly unlikely in an overall convergent setting (e.g., Thompson and Connolly, 1995; Patiño Douce and McCarthy, 1998) and we therefore conclude that the dioritic magmas were derived from enriched lithospheric mantle sources.

5.4. Genesis of magmas forming the southern Granodioritic and northern Granitic Suites

The generation of high-K granodioritic to granitic magmas in convergent settings is commonly attributed to two endmember processes: (1) In continental arc settings, parent mantle melts that are enriched in slab-derived fluids may become contaminated with crustal material during ascent (e.g., DePaolo, 1981; Hildreth and Moorbath, 1988); (2) In syn- to post-collisional settings melting of crustal source rocks may occur as a consequence of decompression following delamination of the lithospheric root or slab breakoff (e.g., Roberts and Clemens, 1993; von Blanckenburg et al., 1998). Although both the SS and the NS were formed from several magma pulses, both complexes show little internal compositional variation and there is almost no compositional overlap between them (e.g., Figs. 2–5). Therefore, an origin by an AFC process (assimilation and combined fractional crystallization; DePaolo, 1981) is regarded as unlikely and a purely crustal origin of the magmas has to be envisaged.

Compositional diversity among crustal magmas may arise in part from different source compositions, but variation of melting conditions, such as H_2O content, pressure, temperature and oxygen fugacity, may play an equally important role (e.g., Wolf and Wyllie, 1994; Gardien et al., 1995; Patiño Douce, 1996; Patiño Douce and Beard, 1995, 1996; Patiño Douce and McCarthy, 1998; Singh and Johannes, 1996; Thompson, 1996; and references therein). Compositional differences of magmas produced by partial melting of different source rocks, such as amphibolites, tonalitic gneisses, metagreywackes and metapelites, under variable melting conditions may

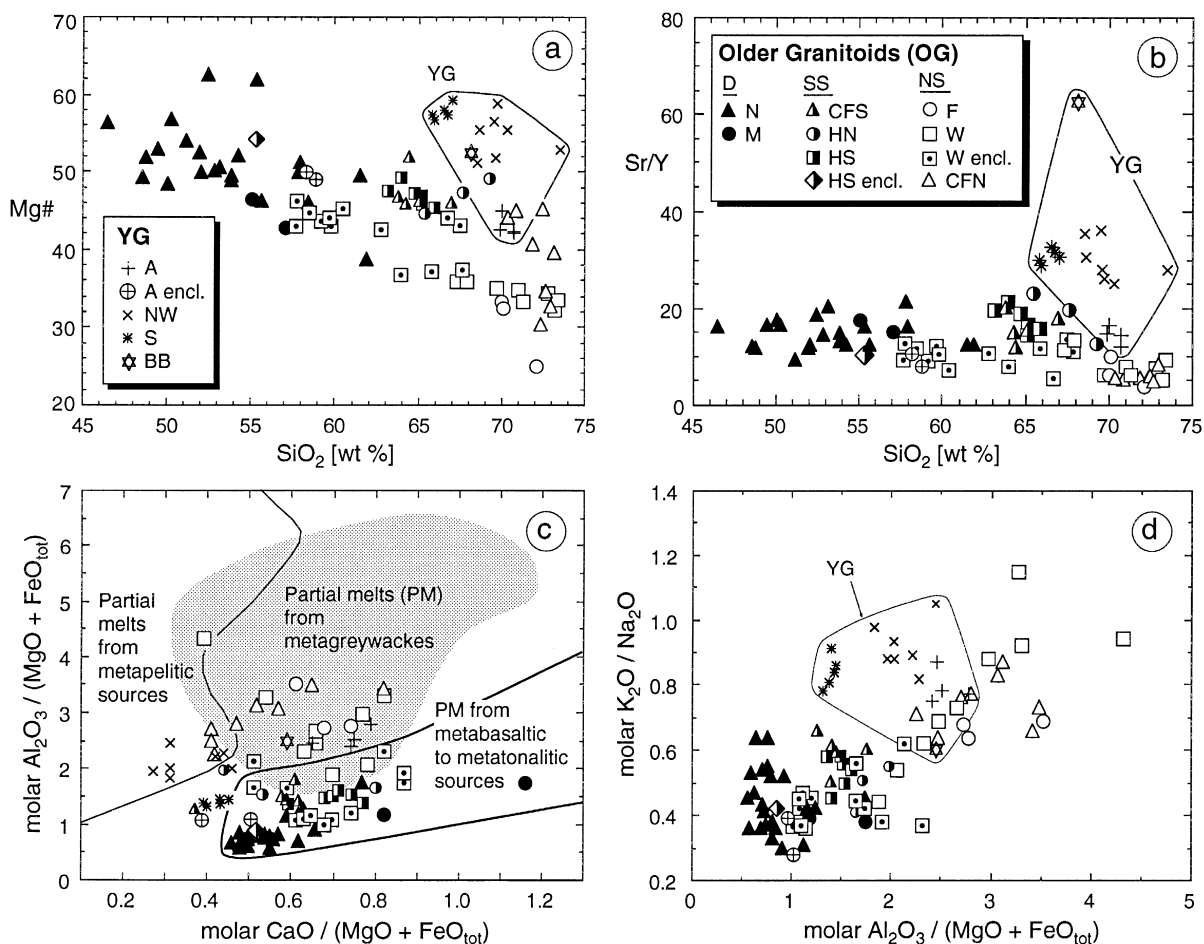


Fig. 7. (a–d) Chemical compositions of I-type granitoids from the northern Vosges and Schwarzwald. (a) Mg# [= molar 100* MgO / (MgO + 0.9FeO_{tot})] vs. SiO₂. Note that for given SiO₂ content, YG samples have higher Mg# than the older granites (NS) and granodiorites (SS). (b) Sr/Y vs. SiO₂. High Sr/Y shown by the YG samples may be due to a higher amount of garnet in the residue during partial melting and segregation in a crustal source. (c) Molar Al₂O₃ / (MgO + FeO_{tot}) vs. molar CaO / (MgO + FeO_{tot}). Outlined fields denote compositions of partial melts obtained in experimental studies by dehydration melting of various bulk compositions (Wolf and Wyllie, 1994; Gardien et al., 1995; Patiño Douce, 1996; Patiño Douce and Beard, 1995, 1996; Patiño Douce and McCarthy, 1998; Singh and Johannes, 1996; Thompson, 1996; and references therein). See text for further explanation. (d) Molar K₂O / Na₂O vs. molar Al₂O₃ / (MgO + FeO_{tot}). Compared with the older granodiorites (SS) and granites (NS), the samples from the YG are displaced towards higher K₂O / Na₂O and/or lower Al₂O₃ / (MgO + FeO_{tot}). See text for discussion.

be visualized in terms of molar oxide ratios, such as K₂O / Na₂O, Al₂O₃ / (MgO + FeO_{tot}) and CaO / (MgO + FeO_{tot}). Partial melts derived from metabasalts and andesites, for example, have lower Al₂O₃ / (MgO + FeO_{tot}) and K₂O / Na₂O, but higher CaO / (MgO + FeO_{tot}) than those derived from metapelites (Fig. 7b and c). On the other hand, the compositions of melts derived from a given source depend on intensive variables during melting. For example, temperature, pressure, H₂O content and

oxygen fugacity control both the degree of partial melting and the stability fields of residual phases (e.g., plagioclase, biotite, orthopyroxene, garnet) that buffer melt compositions (e.g., Patiño Douce, 1996; Patiño Douce and Beard, 1996). As can be seen from Fig. 7c and d, the SS rocks have lower values of Al₂O₃ / (MgO + FeO_{tot}) and K₂O / Na₂O than the NS rocks and their magmas were most likely derived from metaigneous source rocks. The NS granites have chemical characteristics that are more compati-

ble with an origin from metagreywackes. Note, that the SS granodiorites have significantly higher $\varepsilon_{\text{Nd}}(\text{I})$ values than the NS granites (Fig. 6). A significant contribution from metapelitic sources to the SS and NS magmas can be excluded, since their $\text{CaO}/(\text{MgO} + \text{FeO})$ ratios are too high (Fig. 7c).

For the magmas of both complexes the concave-upward shape of the REE patterns suggest that (1) the amphibole-out boundary was not crossed during partial melting leaving amphibole as a major restite phase and (2) garnet was not a major fractionating phase. Compared with the NS granites, the SS granodiorites show higher values of Eu/Eu^* and Sr/Nd and higher abundances of Sr suggesting a smaller amount of feldspar (plagioclase) in their residues during magma segregation.

5.5. Genesis of YG

Samples from the different YG intrusive suites show variable values of $\text{Al}_2\text{O}_3/(\text{MgO} + \text{FeO}_{\text{tot}})$, $\text{K}_2\text{O}/\text{Na}_2\text{O}$ and $\text{CaO}/(\text{MgO} + \text{FeO}_{\text{tot}})$ that in some cases are different from those of the older NS granites (Fig. 7c and d). Such compositional differences may be due to variable source compositions and/or melting conditions. Chemical characteristics of both granitic suites are compatible with a derivation by a relatively high degree of partial melting from metasedimentary sources. Relatively high abundances of Th (up to 44 ppm; Table 3; Fig. 3a) and P_2O_5 (Fig. 3b) in the granites from Natzwiller, Senones and Baden–Baden could be explained by exceptionally high amounts of monazite in their sources. Compared to the NS granites, YG samples tend to have higher $\text{Mg}\#$ at similar SiO_2 (Fig. 7a). This difference is most pronounced for the Senones, Natzwiller and Baden–Baden granites that also show the highest $(\text{Tb}/\text{Yb})_{\text{cn}}$ ratios (Fig. 5). It has been shown that with increasing pressure, the $\text{Mg}\#$ of granitoid partial melts increases relative to the $\text{Mg}\#$ of coexisting garnet and biotite (Patiño Douce, 1996). One may therefore speculate that the YG magmas were generated at greater depths than the NS magmas resulting in a higher amount of residual garnet.

6. Conclusions

In the northern Vosges, early Carboniferous post-accretionary high-K calc-alkaline plutonic activity

started with the intrusion of dioritic magmas that were derived from an enriched lithospheric mantle. Subsequently, several crust-derived magma pulses formed a southern granodioritic and a northern granitic complex. Aside from mafic microgranular enclaves of dioritic to tonalitic composition, both complexes show little internal compositional variation. Microstructures of enclaves and surrounding host rocks indicate the coexistence of mantle-derived dioritic and crust-derived felsic magmas. Chemical and isotopic characteristics of the granodiorites point to a metagneous (metabasitic to metatonalitic) crustal source, whereas the granitic magmas were most probably derived by dehydration melting of metagreywackes. A substantial contribution of metapelitic material to the granodiorites and granites can be ruled out. Abundances and variations of REE, Y, Rb and Sr in granodiorites and granites favour amphibole and plagioclase, but rule out garnet, as major fractionating phases during magma segregation. Trace element characteristics of the OG are consistent with, but do not require magma generation in a volcanic-arc setting above a subducting slab.

The YG of Andlau, Natzwiller and Senones most probably originated by dehydration melting of metasedimentary sources at greater depths, since their trace element characteristics suggest higher amounts of garnet and amphibole as fractionating phases. The granite of Baden–Baden (northern Schwarzwald) shows similar characteristics.

Whereas all the older I-type granitoids (diorites, granodiorites, granites) form elongated WSW–ENE trending complexes, the younger granitic plutons show round shapes suggesting a change in the crustal stress field. Intrusion depths as deduced from Al-in-hornblende barometry tend to decrease in the order of decreasing intrusion age, i.e., from about 10 km (Neuntelstein diorite) to about 3 km (YG).

Acknowledgements

This study is a contribution to the German National Research Project ‘Orogenic processes with particular reference to the Variscides’. Financial support by the Deutsche Forschungsgemeinschaft (Al

166/8) is gratefully acknowledged. Technical support was provided by Heidi Frohna-Binder, Roland Gehann, Hans-Peter Meyer, Charly Wacker (†) and Horst Marschall. We thank Gerhard Eisbacher and Frank Volker for discussions as well as H.-J. Förster and an anonymous reviewer for constructive criticisms of an earlier version of the manuscript.

References

- Ahrendt, H., Clauer, N., Hunziker, J.C., Weber, K., 1983. Migration of folding and metamorphism in the Rheinisches Schiefergebirge deduced from K–Ar and Rb–Sr age determinations. In: Martin, H., Eder, F.W. (Eds.), *Intracontinental Fold Belts*. Springer, Berlin, pp. 323–338.
- Ahrendt, H., Franzke, H.J., Marheine, D., Schwab, M., Wemmer, K., 1996. Zum Alter der Metamorphose in der Wippraer Zone/Harz — Ergebnisse von K/Ar-Altersdatierungen an schwachmetamorphen Sedimenten. *Z. Geol. Ges.* 147, 39–56.
- Allen, C.M., 1991. Local equilibrium of mafic enclaves and granitoids of the Turtle pluton southeastern California: mineral, chemical and isotopic evidence. *Am. Mineral.* 76, 574–588.
- Altherr, R., Lugovic, B., Meyer, H.-P., Majer, V., 1995. Early Miocene post-collisional calc-alkaline magmatism along the easternmost segment of the Periadriatic fault system (Slovenia and Croatia). *Mineral. Petrol.* 54, 225–247.
- Altherr, R., Henes-Klaiber, U., Hegner, E., Satir, M., Langer, C., 1999. Plutonism in the Variscan Odenwald (Germany): from subduction to collision. *Geol. Rundschau*, in press.
- Anderle, H.J., Massonne, H.-J., Meisl, J., Oncken, O., Weber, K., 1990. Southern Taunus Mountains. Terranes in the Circum-Atlantic Paleozoic Orogens (IGCP 233), Field Guide: Rhenohercynian Belt and Mid-German Crystalline Rise. Göttingen, pp. 125–148.
- Bachtadse, V., Torsvik, T.H., Tait, J.A., Soffel, H.C., 1995. X. Paleomagnetic constraints on the paleogeographic evolution of Europe during the Paleozoic. In: Dallmeyer, R.D., Franke, W., Weber, K. (Eds.), *Pre-Permian Geology of Central and Eastern Europe*. Springer, Berlin, pp. 567–578.
- Baker, D.R., 1989. Tracer versus trace element diffusion: diffusional decoupling of Sr concentration from Sr isotope composition. *Geochim. Cosmochim. Acta* 53, 3015–3023.
- Bedard, L.P., Barnes, S.-J., 1990. Instrumental neutron activation analysis by collecting only one spectrum: results for international geochemical reference samples. *Geostand. Newsl.* 14, 479–484.
- Bergantz, G.W., 1989. Underplating and partial melting: implications for melt generation and extraction. *Science* 245, 1093–1094.
- Bernard-Griffiths, J., Peucat, J.J., Sheppard, S., Vidal, P., 1985. Petrogenesis of Hercynian leucogranites from the southern Armorican Massif: contribution of REE and isotopic (Sr, Nd, Pb and O) geochemical data to the study of source rock characteristics and ages. *Earth Planet. Sci. Lett.* 74, 235–250.
- Boutin, R., Montigny, R., Thuizat, R., 1995. Chronologie K–Ar et ³⁹Ar–⁴⁰Ar du métamorphisme et du magmatisme des Vosges. Comparaison avec les massifs varisques avoisinants. *Géol. Fr.* 1, 3–25.
- Boynton, W.V., 1984. Cosmochemistry of the rare earth elements: meteorite studies. In: Henderson, P. (Ed.), *Rare Earth Element Geochemistry*. Elsevier, Amsterdam, pp. 63–114.
- Brown, M., 1993. *P–T–t* evolution of orogenic belts and the causes of regional metamorphism. *J. Geol. Soc. (London)* 150, 227–241.
- Class, C., Altherr, R., Volker, F., Eberz, G., McCulloch, M.T., 1994. Petrogenesis of Pliocene to Quaternary alkali basalts from the Huri Hills, northern Kenya. *Chem. Geol.* 113, 1–22.
- Clauer, N., Bonhomme, M., 1970. Datations rubidium–strontium dans les schistes de Steige et la série de Villé (Vosges). *Bull. Serv. Carte Géol. Alsace Lorraine* 23, 191–208.
- de Béthune, P., Lapania, E., Rousseau-Turay, M., Eller von, J.P., 1968. Les diorites du Neuntelstein et du Neugrunrain près du Hohwald (Vosges), et leurs enclaves. *Bull. Serv. Carte Géol. Alsace Lorraine* 21, 23–44.
- de la Roche, H., Eller von, J.P., 1969. Caractères et tendances géochimiques des bandes granodioritiques et granitiques formant le massif du Champ-du-Feu (Vosges cristallines du Nord). *Bull. Serv. Carte Géol. Alsace Lorraine* 22, 199–233.
- DePaolo, D.J., 1981. Trace element and isotopic effects of combined wall rock assimilation and fractional crystallization. *Earth Planet. Sci. Lett.* 53, 189–202.
- Didier, J., 1991. The various types of enclaves in the Hercynian granitoids of the Massif Central, France. In: Didier, J., Barbarin, B. (Eds.), *Enclaves and Granite Petrology. Developments in Petrology*, Vol. 13. Elsevier, Amsterdam, pp. 47–62.
- Doubinger, J., 1963. Chitinozoaires ordoviciens et siluriens des schistes de Steige dans les Vosges. *Bull. Serv. Carte Géol. Alsace Lorraine* 16, 125–136.
- Echtler, H.P., Altherr, R., 1993. Variscan crustal evolution in the Vosges Mountains and in the Schwarzwald: guide to the excursion of the Swiss Geological Society and the Swiss Society of Mineralogy and Petrology (3–5 October, 1992). *Schweiz. Mineral. Petrogr. Mitt.* 73, 113–128.
- Edel, J.B., Montigny, R., Royer, J.Y., Thuizat, R., Troland, F., 1986. Paleomagnetic investigations and K–Ar dating on the Variscan plutonic massif of the Champ du Feu and its volcanic-sedimentary environment, northern Vosges, France. *Tectonophysics* 122, 165–185.
- Eisbacher, G.H., Lüschen, E., Wickert, F., 1989. Crustal-scale thrusting and extension in the Hercynian Schwarzwald and Vosges, Central Europe. *Tectonics* 8, 1–21.
- Elburg, M.A., 1996. Evidence of isotopic equilibration between microgranitoid enclaves and host granodiorite, Warburton Granodiorite, Lachlan Fold Belt, Australia. *Lithos* 38, 1–22.
- Faul, H., Jäger, E., 1963. Age of some granitic rocks in the Vosges, the Schwarzwald and the Massif Central. *J. Geophys. Res.* 68, 3293–3300.
- Finger, F., Roberts, M.P., Haunschild, B., Schermaier, A., Steyrer, H.P., 1997. Variscan granitoids of Central Europe: their typology, potential sources and tectonothermal relations. *Mineral. Petrol.* 61, 67–96.
- Fluck, P., 1980. Métamorphisme et magmatisme dans les Vosges moyennes d'Alsace. *Sci. Géol. Bull.* 62, 1–248.

- Fluck, P., Edel, J.-B., Gagny, C., Montigny, R., Piqué, A., Schneider, J.-L., Whitechurch, H., 1989. Carte synthétique et géotransverse N–S de la chaîne varisque des Vosges (France). Synthèse des travaux effectués depuis deux décennies. C. R. Acad. Sci. Paris 309, 907–912, Sér. II.
- Franke, W., 1995. III.B.1. Stratigraphy. In: Dallmeyer, R.D., Franke, W., Weber, K. (Eds.), *Pre-Permian Geology of Central and Eastern Europe*. Springer, Berlin, pp. 33–49.
- Franke, W., Dallmeyer, R.D., Weber, K., 1995. XI. Geodynamic evolution. In: Dallmeyer, R.D., Franke, W., Weber, K. (Eds.), *Pre-Permian Geology of Central and Eastern Europe*. Springer, Berlin, pp. 579–593.
- Galán, G., Pin, C., Duthou, J.-L., 1996. Sr–Nd isotopic record of multi-stage interactions between mantle-derived magmas and crustal components in a collision context — the ultramafic-granitoid association from Vivero (Hercynian belt, NW Spain). *Chem. Geol.* 131, 67–91.
- Ganssloser, M., Theye, T., Wachendorf, H., 1996. Detrital glauconite in graywackes of the Rhenohercynian Harz mountains and the geodynamic implications. *Geol. Rundsch.* 85, 755–760.
- Garbe-Schönberg, C.-D., 1993. Simultaneous determination of thirty-seven trace elements in twenty-eight international rocks standards by ICP-MS. *Geostand. Newsl.* 17, 81–97.
- Gardien, V., Thompson, A.B., Grujic, D., Ulmer, P., 1995. Experimental melting of biotite + plagioclase + quartz \pm muscovite assemblages and implications for crustal melting. *J. Geophys. Res.* 100, 15581–15591.
- Govindaraju, K., Roelandts, K., 1989. 1988 compilation report on trace elements in six ANRT rock reference samples: diorite DR-N, serpentine UB-N, bauxite BX-N, disthene DT-N, granite GS-N and potash feldspar FK-N. *Geostand. Newsl.* 13, 5–67.
- Hahn-Weinheimer, P., Propach, G., Raschka, H., 1971. Zur Genese des Kagenfels Granits (Nordvogesen). *Bull. Serv. Carte Géol. Alsace Lorraine* 24, 5–56.
- Hegner, E., Roddick, C.R., Fortier, S.M., Hulbert, L., 1995. Nd, Sr, Pb, Ar and O isotope systematics of Sturgeon Lake kimberlite, Saskatchewan, Canada: constraints on emplacement age, alteration, and source composition. *Contrib. Mineral. Petrol.* 120, 212–222.
- Hess, J.C., Lippolt, H.J., Kober, B., 1995. The age of the Kagenfels granite (northern Vosges) and its bearing on the intrusion scheme of late Variscan granitoids. *Geol. Rundsch.* 84, 568–577.
- Hildreth, W., Moorbath, S., 1988. Crustal contributions to arc magmatism in the Andes of Central Chile. *Contrib. Mineral. Petrol.* 98, 455–489.
- Hoefs, J., Emmermann, R., 1983. The oxygen isotope composition of Hercynian granites and pre-Hercynian gneisses from the Schwarzwald, SW Germany. *Contrib. Mineral. Petrol.* 83, 320–329.
- Holden, P., Halliday, A.N., Stephens, W.E., Henney, P.J., 1991. Chemical and isotopic evidence for major mass transfer between mafic enclaves and felsic magma. *Chem. Geol.* 92, 135–152.
- Holub, F.V., Klecka, M., Matejka, D., 1995. VII.C.3. Igneous activity. In: Dallmeyer, R.D., Franke, W., Weber, K. (Eds.), *Pre-Permian Geology of Central and Eastern Europe*. Springer, Berlin, pp. 444–452.
- Huppert, H.E., Sparks, R.S.J., 1988. The generation of granitic magmas by intrusion of basalt into continental crust. *J. Petrol.* 29, 599–624.
- Janousek, V., Rogers, G., Bowes, D.R., 1995. Sr–Nd isotopic constraints on the petrogenesis of the Central Bohemian Pluton, Czech Republic. *Geol. Rundsch.* 84, 520–534.
- Kalt, A., Hanel, M., Schleicher, H., Kramm, U., 1994. Petrology and geochronology of eclogites from the Variscan Schwarzwald (F.R.G.). *Contrib. Mineral. Petrol.* 115, 287–302.
- Kossmat, F., 1927. Gliederung des varistischen Gebirgsbaus. *Abh. Sächs. Geol. Landesamt* 1, 1–39.
- Krohe, A., Eisbacher, G.H., 1988. Oblique crustal detachment in the Variscan Schwarzwald, southwestern Germany. *Geol. Rundsch.* 77, 25–45.
- Leshner, C.E., 1994. Kinetics of Sr and Nd exchange in silicate liquids: theory, experiments, and applications to uphill diffusion, isotopic equilibration, and irreversible mixing of magmas. *J. Geophys. Res.* 99, 9585–9604.
- Leterrier, J., 1978. Aspects chimiques des interactions entre les magmas basiques et leur encaissant pélique dans le plutonisme. *Bull. Soc. Géol. Fr.* 20, 21–28.
- Massonne, H.-J., 1995. III.C.4. Metamorphic evolution. In: Dallmeyer, R.D., Franke, W., Weber, K. (Eds.), *Pre-Permian Geology of Central and Eastern Europe*. Springer, Berlin, pp. 132–137.
- Mehl, J., 1988. Biostratigraphische Datierung des nordschwarzwälder metamorphen Paläozoikums mit Hilfe moderner Röntgenuntersuchungen, Vortrag 4. Rundgespräch Variszikum, Heidelberg.
- Meisl, S., 1990. Metavolcanic rocks in the ‘northern Phyllite Zone’ at the southern margin of the Rhenohercynian Belt. Terranes in the Circum-Atlantic Paleozoic Orogens (IGCP 233), Field Guide: Rhenohercynian Belt and Mid-German Crystalline Rise. Göttingen, pp. 25–42.
- Meisl, S., Anderle, H.-J., Strecker, G., 1982. Niedrigtemperierte Metamorphose im Taunus und im Soonwald. *Fortschr. Mineral., Beih.* 60 (2), 43–69.
- Metcalfe, R.V., Smith, E.I., Walker, J.D., Reed, R.C., Gonzales, D.A., 1995. Isotopic disequilibrium among commingled hybrid magmas: Evidence for a two-stage magma mixing-commingling process in the Mt. Perkins Pluton, Arizona. *J. Geol.* 103, 509–527.
- Müller, H.D., 1989. Geochemistry of metasediments in the Hercynian and pre-Hercynian crust of the Schwarzwald, the Vosges and northern Switzerland. *Tectonophysics* 157, 97–108.
- Oncken, O., 1997. Transformation of a magmatic arc and an orogenic root during oblique collision and its consequences for the evolution of the European Variscides (Mid-German Crystalline Rise). *Geol. Rundsch.* 86, 2–20.
- Patiño Douce, A.E., 1996. Effects of pressure and H₂O content on the composition of primary crustal melts. *Trans. R. Soc. Edinburgh: Earth Sci.* 87, 11–21.
- Patiño Douce, A.E., Beard, J.S., 1995. Dehydration-melting of biotite gneiss and quartz amphibolite from 3 to 15 kbar. *J. Petrol.* 36, 707–738.

- Patiño Douce, A.E., Beard, J.S., 1996. Effects of P, $f(\text{O}_2)$ and Mg/Fe ratio on dehydration melting of model metagreywackes. *J. Petrol.* 37, 999–1024.
- Patiño Douce, A.E., McCarthy, T.C., 1998. Melting of crustal rocks during continental collision and subduction. In: Hacker, B.R., Liou, J.G. (Eds.), *When Continents Collide: Geodynamics and Geochemistry of Ultrahigh-Pressure Rocks*. Petrology and Structural Geology, Vol. 10. Kluwer Academic Publishers, Dordrecht, pp. 27–55.
- Pearce, J.A., 1996. Source and setting of granitic rocks. *Episode* 19, 120–125.
- Peccerillo, A., Taylor, S.R., 1976. Geochemistry of Eocene calc-alkaline volcanic rocks from the Kastamonu area, northern Turkey. *Contrib. Mineral. Petrol.* 58, 63–81.
- Petford, N., Paterson, B., McCaffrey, K., Pugliese, S., 1996. Melt infiltration and advection in microdioritic enclaves. *Eur. J. Mineral.* 8, 405–412.
- Pin, C., Binon, M., Belin, J.M., Barbarin, B., Clemens, J.D., 1990. Origin of microgranular enclaves in granitoids: equivocal Sr–Nd evidence from Hercynian Rocks in the Massif Central (France). *J. Geophys. Res.* 95, 17821–17828.
- Poli, G., Tommasini, S., Halliday, A.N., 1996. Trace element and isotopic exchange during acid–basic magma interaction processes. *Trans. R. Soc. Edinburgh: Earth Sci.* 87, 225–232.
- Rapp, R.P., 1995. Amphibole-out phase boundary in partially melted metabasalt, its control over liquid fraction and composition, and source permeability. *J. Geophys. Res.* 100, 15601–15610.
- Rapp, R.P., Watson, E.B., 1995. Dehydration melting of metabasalt at 8–32 kbar: implications for continental growth and crust–mantle recycling. *J. Petrol.* 36, 891–931.
- Reddy, G.R., Pant, D.R., 1993. La, Ce, Sm, Eu, Tb, Yb and Lu content of fifteen French geochemical reference samples determined by neutron activation analysis. *Geostand. Newsl.* 17, 113–116.
- Reitz, E., Wickert, F., 1989. Late Cambrian to Early Ordovician acritarchs from the Villé Unit, northern Vosges Mountains (France). *N. Jb. Geol. Paläontol. Mh.* 1989, 375–384.
- Rizki, A., Baroz, F., 1988. Le volcanisme tholéitique du massif de Schirmeck (Vosges septentrionales, France), témoin d'une zone de convergence de plaques au Paléozoïques supérieur. *C. R. Acad. Sci. Paris* 307, 511–516, Sér. II.
- Roberts, M.P., Clemens, J.D., 1993. Origin of high-potassium, calc-alkaline, I-type granitoids. *Geology* 21, 825–828.
- Rock, N.M.S., Gaskarth, J.W., Rundle, C.C., 1986. Late Caledonian dyke-swarms in southern Scotland: a regional zone of primitive K-rich lamprophyres and associated vents. *J. Geol.* 94, 505–522.
- Romick, J.D., Kay, S.M., Kay, R.M., 1992. The influence of amphibole fractionation on the evolution of calc-alkaline andesite and dacite tephras from the central Aleutians, Alaska. *Contrib. Mineral. Petrol.* 112, 101–118.
- Sabatier, H., 1991. Vaugnerites: special lamprophyre-derived mafic enclaves in some Hercynian granites from Western and Central Europe. In: Didier, J., Barbarin, B. (Eds.), *Enclaves and Granite Petrology*. Developments in Petrology Vol. 13. Elsevier, Amsterdam, pp. 63–82.
- Schaltegger, U., 1997. Magma pulses in the Central Variscan Belt: episodic melt generation and emplacement during lithospheric thinning. *Terra Nova* 9, 242–245.
- Schmidt, M.W., 1992. Amphibole composition in tonalite as a function of pressure: an experimental calibration of the Al–hornblende barometer. *Contrib. Mineral. Petrol.* 110, 304–310.
- Singh, J., Johannes, W., 1996. Dehydration melting of tonalites: Part II. Composition of melts and solids. *Contrib. Mineral. Petrol.* 125, 26–44.
- Streckeisen, A.L., 1976. To each plutonic rock its proper name. *Earth Sci. Rev.* 12, 1–33.
- Tait, J.A., Bachtadse, V., Franke, W., Soffel, H.C., 1997. Geodynamic evolution of the European Variscan fold belt: palaeomagnetic and geological constraints. *Geol. Rundsch.* 86, 585–598.
- Thompson, A.B., 1996. Fertility of crustal rocks during anatexis. *Trans. R. Soc. Edinburgh: Earth Sci.* 87, 1–10.
- Thompson, A.B., Connolly, A.D., 1995. Melting of the continental crust: some thermal and petrological constraints on anatexis in continental collision zones and other tectonic settings. *J. Geophys. Res.* 100, 15565–15579.
- Tobschall, H.J., 1975. Geochemische Untersuchungen zum stofflichen Bestand und Sedimentationsmilieu paläozoischer mariner Tone: Ni, Cu, Zn, Rb, Sr, Y, Zr, Nb und Ba in den Steiger Schiefer (Vogesen). *Chem. Erde* 34, 105–167.
- Turpin, L., Velde, D., Pinte, G., 1988. Geochemical comparison between minettes and kersantites from the Western European Hercynian orogen: trace element and Pb–Sr–Nd isotope constraints on their origin. *Earth Planet. Sci. Lett.* 87, 73–86.
- van der Laan, S.R., Wyllie, P.J., 1993. Experimental interaction of granitic and basaltic magmas and implications for mafic enclaves. *J. Petrol.* 34, 491–517.
- Verma, S.P., 1991. Determination of thirteen rare-earth elements by high-performance liquid chromatography in thirty and of K, Rb, Cs, Sr and Ba by isotope dilution mass spectrometry in eighteen international geochemical reference samples. *Geostand. Newsl.* 15, 129–134.
- Verma, S.P., Besch, T., Guevara, M., Schulz-Dobrick, B., 1992. Determination of twelve trace elements in twenty-seven and ten major elements in twenty-three geochemical reference samples by X-ray fluorescence spectrometry. *Geostand. Newsl.* 16, 301–309.
- Vernon, R.H., 1990. Crystallization and hybridism in microgranitoid enclave magmas: microstructural evidence. *J. Geophys. Res.* 95, 17849–17859.
- von Blanckenburg, F., Kagami, H., Deutsch, A., Oberli, F., Meier, M., Wiedenbeck, M., Barth, S., Fischer, H., 1998. The origin of Alpine plutons along the Periadriatic Lineament. *Schweiz. Mineral. Petrogr. Mitt.* 78, 55–66.
- von Eller, J.P., 1964. Dioritisation, granitisation et métamorphisme dans les Vosges cristallines du Nord: I. Région comprise entre la plaine d'Alsace, d'Andlau à Saint-Nabor, et le Champ-du-Feu. *Bull. Serv. Carte Géol. Alsace Lorraine* 17, 171–210.
- von Eller, J.P., 1965. Granitisation, dioritisation et métamorphisme dans les Vosges cristallines du Nord: II. La région comprise entre la faille vosgienne à l'Est de Grendelbruch et

- la vallée de la Bruche à la hauteur de Fouday-Rothau. Bull. Serv. Carte Géol. Alsace Lorraine 18, 117–143.
- von Eller, J.P., 1968. Granitisation, dioritisation et métamorphisme dans les Vosges cristallines du Nord: IV. La zone comprise entre Saales et Denipaire. Bull. Serv. Carte Géol. Alsace Lorraine 21, 3–22.
- von Eller, J.P., 1969. Granitisation, dioritisation et métamorphisme dans les Vosges cristallines du Nord: V. Le massif d'Étival. Bull. Serv. Carte Géol. Alsace Lorraine 22, 185–198.
- von Eller, J.P., Blanalt, J.G., Hameurt, J., Hollinger, J., 1970. Carte géologique du socle vosgien, partie septentrionale. Bull. Serv. Carte Géol. Alsace Lorraine 23, 5–28.
- von Eller, J.P., Hameurt, J., Ruhland, M., 1971a. Évolutions métamorphiques et ignées dans les Vosges. C. R. Soc. Géol. Fr. 1971, 296–306.
- von Eller, J.P., Lapania, E., Laduron, D., Béthune de, P., 1971b. Caractères polymétamorphiques des cornéennes de la région de Barr Andlau (Vosges). Bull. Serv. Carte Géol. Alsace Lorraine 24, 127–148.
- Watkins, P.J., Nolan, J., 1990. Determination of rare-earth elements, scandium, yttrium and hafnium in 32 geochemical reference materials using inductively coupled plasma-atomic emission spectrometry. *Geostand. Newsl.* 14, 11–20.
- Wickert, F., Eisbacher, G.H., 1988. Two-sided Variscan thrust tectonics in the Vosges Mountains, northeastern France. *Geodin. Acta* (Paris) 2, 101–120.
- Wickert, F., Altherr, R., Deutsch, M., 1990. Polyphase Variscan tectonics and metamorphism along a segment of the Saxothuringian–Moldanubian boundary: the Baden–Baden Zone, northern Schwarzwald (F.R.G.). *Geol. Rundsch.* 79, 627–647.
- Wolf, M.B., Wyllie, J.P., 1994. Dehydration-melting of amphibolite at 10 kbar: the effects of temperature and time. *Contrib. Mineral. Petrol.* 115, 369–383.
- Zorpi, M.J., Coulon, C., Orisini, J.B., Cocirta, C., 1989. Magma mingling, zoning and emplacement in calc-alkaline granitoid plutons. *Tectonophysics* 157, 315–329.
- Zorpi, M.J., Coulon, C., Orisini, J.B., 1991. Hybridization between felsic and mafic magmas in calc-alkaline granitoids — a case study in northern Sardinia, Italy. *Chem. Geol.* 92, 45–86.